

This is the peer reviewed version of the following article:

Designing Chimeric Molecules for Drug Discovery by Leveraging Chemical Biology / Borsari, C.; Trader, D. J.; Tait, A.; Costi, M. P.. - In: JOURNAL OF MEDICINAL CHEMISTRY. - ISSN 0022-2623. - 63:5(2020), pp. 1908-1928. [[10.1021/acs.jmedchem.9b01456](https://doi.org/10.1021/acs.jmedchem.9b01456)]

*Terms of use:*

The terms and conditions for the reuse of this version of the manuscript are specified in the publishing policy. For all terms of use and more information see the publisher's website.

03/05/2026 15:34

(Article begins on next page)

# 1 Designing Chimeric Molecules for Drug Discovery by Leveraging 2 Chemical Biology

3 Chiara Borsari, Darci J. Trader, Annalisa Tait, and Maria P. Costi\*



Cite This: <https://dx.doi.org/10.1021/acs.jmedchem.9b01456>



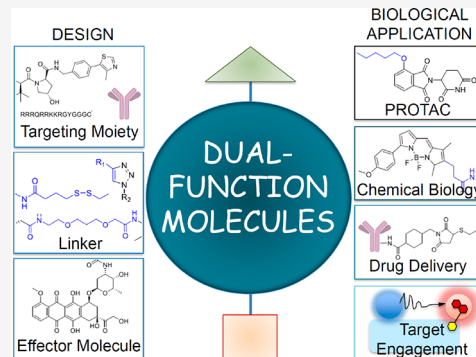
Read Online

ACCESS |

Metrics & More

Article Recommendations

4 **ABSTRACT:** After the first seed concept introduced in the 18th century, different  
5 disciplines have attributed different names to dual-functional molecules depending  
6 on their application, including bioconjugates, bifunctional compounds, multi-  
7 targeting molecules, chimeras, hybrids, engineered compounds. However, these  
8 engineered constructs share a general structure: a first component that targets a  
9 specific cell and a second component that exerts the pharmacological activity. A  
10 stable or cleavable linker connects the two modules of a chimera. Herein, we  
11 discuss the recent advances in the rapidly expanding field of chimeric molecules  
12 leveraging chemical biology concepts. This Perspective is focused on bifunctional  
13 compounds in which one component is a lead compound or a drug. In detail, we  
14 discuss chemical features of chimeric molecules and their use for targeted delivery  
15 and for target engagement studies.



## 1. INTRODUCTION

16 A chimeric molecule is an engineered construct in which two or  
17 more components are linked to form a novel biological agent.  
18 Chimeric molecules can be considered as variants of an idea  
19 proposed by Paul Ehrlich in the late 1800s. This concept  
20 describes a bifunctional molecule in which one component  
21 targets the molecule to a specific cell and the second component  
22 exerts a pharmacological activity.<sup>1,2</sup> Different disciplines have  
23 attributed multiple names to dual-functional molecules  
24 (chimeras, hybrids, bioconjugates, bifunctional compounds,  
25 multitargeting molecules, engineered compounds) depending  
26 on the field of application, but the general structure is conserved.  
27 Recently, the knowledge in cellular and molecular biology  
28 widely increased. The chemical biology field allowed the  
29 application of the chemistry knowledge to deliver specific  
30 biomolecules on the cell membrane and into the cells. The  
31 concepts of chemical biology were translated into drug discovery  
32 of chimeric molecules (or chimeras).<sup>3,4</sup> These entities display (i)  
33 a targeting moiety and (ii) an effector molecule within the same  
34 chemical construct, and their individual function could be  
35 largely modulated with appropriate conjugation chemistry  
36 strategies where a linker is the bridging element (Figure 1).<sup>1,3</sup>  
37 Recently, the exploitation of these systems for drug delivery  
38 implementation, particularly into cancer cells, has been  
39 reviewed.<sup>4</sup>

40 This Perspective discusses the recent advances in the rapidly  
41 expanding field of chimeric molecules in which one component  
42 is a lead compound or a drug. In detail we discuss chemical  
43 features of chimeric molecules, targeted delivery, and the

exploitation of chimeric molecules for target engagement 44  
studies. 45

Section 2 is focused on linker chemistry. To develop small 46  
molecules that engage a specific cell type or protein target, a 47  
small molecule needs to be linked with another moiety that 48  
allows selective target recognition. The linker plays a pivotal role 49  
in the development of chimeric compounds and allows bridging 50  
of two pharmacophores within one molecule. The type and the 51  
length of the linker are essential parameters for the design and 52  
biological activity of chimeras, leading to a rapid expansion of 53  
the linker chemistry field. 54

Section 3 deals with drug delivery based on receptor-mediated 55  
endocytosis (RME). Cell membrane permeation represents the 56  
major bottleneck in achieving the sufficient drug concentration 57  
for therapeutic effect. Drug delivery systems exploiting receptor- 58  
mediated endocytosis have been proposed as a promising tool to 59  
overcome tissue barriers and have given an important 60  
contribution to medical practice, especially in the area of cancer 61  
and central nervous system (CNS) disorders. Three classes of 62  
ligands have been used to target receptors at the cell membrane 63  
and are herein discussed: (i) cell-penetrating peptides (CPPs), 64  
(ii) tumor homing peptides, and (iii) monoclonal antibodies. 65

Section 4 covers the recent advancements in chimeric 66  
molecules engineered to demonstrate how a drug engages its 67

**Special Issue:** Women in Medicinal Chemistry

**Received:** September 1, 2019

**Published:** February 5, 2020

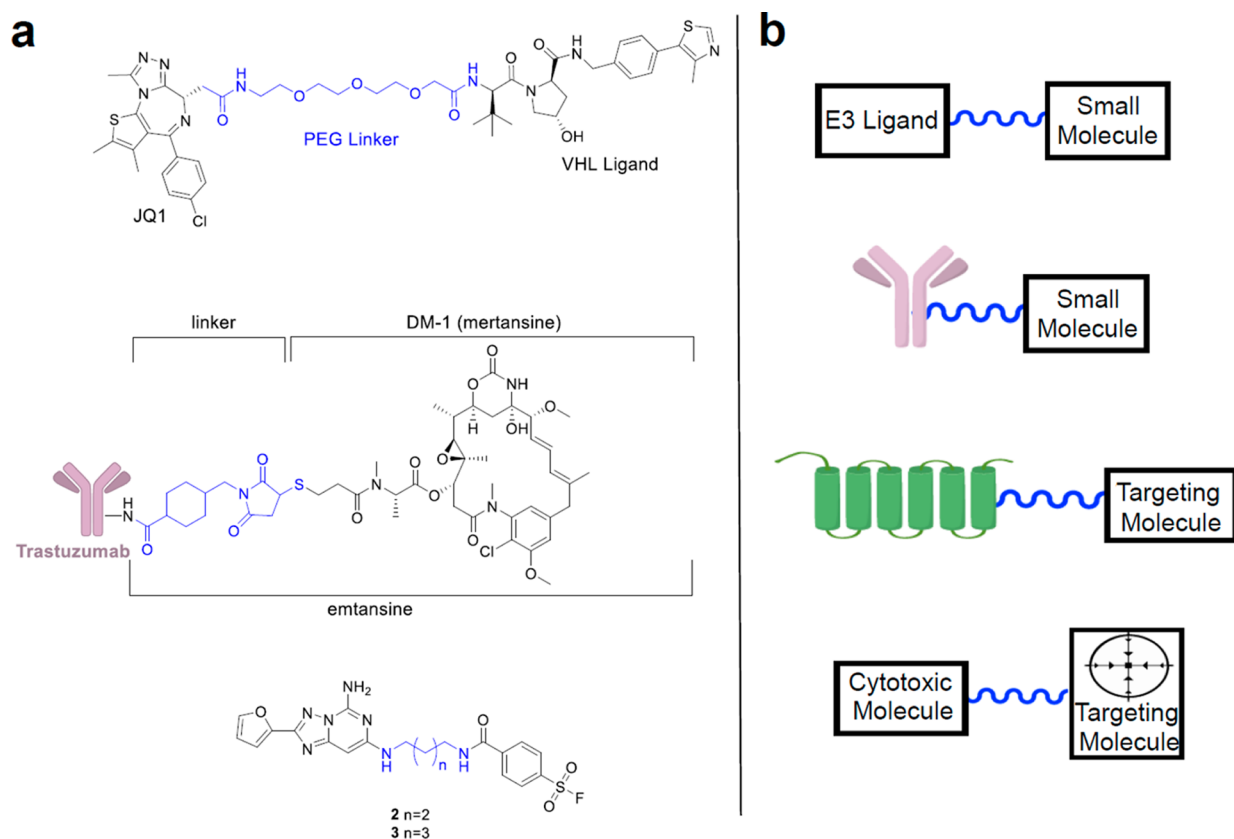


**Figure 1.** Overview of chimeric compounds with a diversity of structures: (a) examples of chimeras discussed in the Perspective, where linker moiety is highlighted in blue; (b) general structures of chimeric compounds.

own target intracellularly. Herein, we discuss the crucial integration of chemical biology knowledge, drug discovery strategies, and medicinal chemistry to foster structure–mechanism of action studies and subsequent structural modifications.

## 2. LINKER FEATURES IN THE MODULAR APPROACH TO CHIMERIC COMPOUNDS

**2.1. Linker Chemistry.** Physically connecting two chemical moieties or a small molecule with a protein occurs through a moiety called linker. A wide variety of linkers have been developed that consider if the target of the small molecule is intra- or extracellular and what type of cell or tissue the small molecule needs to target. If the desired target is intracellular, typically the linker includes a moiety that can be cleaved once the chimera is inside the cell. Linkers also play an important role in activity-based protein profiling experiments.

A commonly used linker type is hydrazone, **Figure 2a**. The hydrazone moiety can typically be easily installed because of its compatibility with peptide synthesis.<sup>5</sup> The hydrazone moiety is stable at physiological pH and cleaves at an acidic pH, but additional conditions that do not require acids have been developed.<sup>6</sup> While the hydrazone moiety has been widely used in diversity-oriented synthesis<sup>7</sup> and as an additional handle in peptide synthesis,<sup>8</sup> more recently it has been exploited as a reversible linker for proteomics experiments.<sup>9</sup> Several different types have been developed, including an acyl hydrazone from the Kohn laboratory.<sup>10</sup> Their study highlights a more efficient capture and release of the targeted protein pool as compared to standard protocols due to the mild conditions for the hydrazone release. Captured proteins do not have to be exposed to SDS or 8

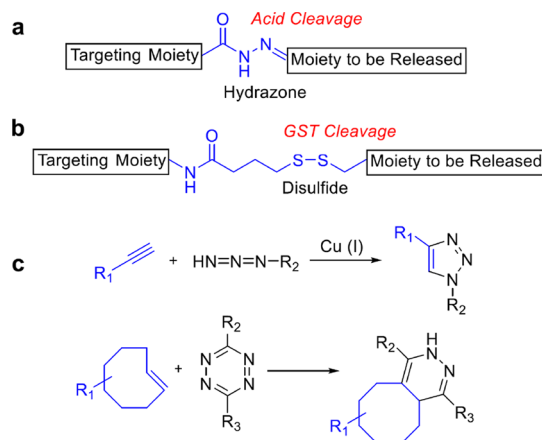


**Figure 2.** Examples of linkers and cleavage conditions: (a) hydrazone; (b) disulfide linker; (c) traditional click chemistry reaction used to easily link moieties together. The inverse Diels–Alder reaction has been used to link molecules to a solid surface for screening or for the release of a cytotoxic moiety. Linkers are highlighted in blue.

M guanidine to release them for mass spectrometry experiments. The Dawson group developed a bisaryl hydrazone linker also highlighting the mild conditions that can be exploited to release captured proteins from a hydrazone-linked molecule.<sup>11</sup>

The disulfide moiety is also commonly investigated in chemical biology (**Figure 2b**). It has been highly utilized to cyclize peptides. The cyclization of peptides has been shown to increase their resistance to proteases and, in some cases, stabilizes the structure to boost its ability to bind to the targeted protein.<sup>12</sup> More recent trends have promoted the concept of 106

107 peptide stapling rather than disulfide bonds because of the  
108 reversibility of the disulfide bond.<sup>13</sup> Nonetheless, disulfides in  
109 peptide therapeutics are still common, with the most well-  
110 known therapeutic peptide that incorporates disulfide bonds  
111 being insulin.<sup>14</sup> Disulfide linkers have also been exploited in  
112 recombinant fusion proteins<sup>15</sup> and for the synthesis of peptide  
113 libraries.<sup>16,17</sup>

114 Since the disulfide linker bond can be reversed under  
115 physiological conditions, it has been integrated into drug  
116 delivery approaches and in prodrug scaffolds. Cells have a high  
117 level of free -SH moieties in their cytosol. Once the disulfide-  
118 linked drug enters the cytosol, the disulfide can be reduced,  
119 releasing the drug moiety.<sup>18</sup> The disulfide linker has been  
120 extensively used in the conjugation of small molecules to  
121 antibodies. Anticancer drugs, including doxorubicin (**1**),  
122 methotrexate, and mitomycin C, have been linked to antibodies  
123 and, after internalization, the disulfide linker is cleaved and the  
124 cytotoxic agent released.<sup>19</sup> This method increases the uptake of  
125 the cytotoxic drug by cancer cells and not by the healthy ones. A  
126 linker containing a free thiol is conjugated to the small molecule  
127 of interest at a location that does not affect its activity. This  
128 entire moiety is then bound to an antibody through generation  
129 of a disulfide bond between the free thiol linked to the small  
130 molecule and a cysteine residue on the antibody.

131 Other linkers used in chemical biology can be generated  
132 through the reaction commonly referred to as click chemistry  
133 (Figure 2c). The term click chemistry, coined by Karl Barry  
134 Sharpless, refers to a variety of reactions that are considered  
135 simple and regiospecific and provide high yields.<sup>20</sup> However,  
136 click chemistry has become traditionally referred to as the  
137 Huisgen 1,3-dipolar cycloaddition of azides and terminal  
138 alkynes. The most basic click reaction, with copper as a catalyst,  
139 produces a 1,4-substituted triazole. This reaction has been used  
140 to (i) link natural products to tags aiding in identification and  
141 detection,<sup>21,22</sup> (ii) introduce a biotin moiety on proteins of  
142 interest for enrichment for mass spectrometry experiments,<sup>23–26</sup>  
143 and (iii) synthesize a variety of small molecule libraries on solid-  
144 phase or polymer-like structures.<sup>27–30</sup> A click reaction  
145 generating a releasable linker is the inverse-electron-demand  
146 Diels–Alder between a conjugated trans-cyclooctene and a  
147 tetrazine moiety. This type of cleavage linker has been  
148 demonstrated to effectively release **1** or other ligands conjugated  
149 to an antibody.<sup>31,32</sup> The Garner laboratory has also employed  
150 this type of click reaction to develop different platforms for the  
151 screening of small molecule binders to RNA.<sup>33,34</sup>

152 The linkers described here are just a few of those that have  
153 been developed to help answer a variety of chemical biology  
154 questions and for therapeutic application. In the remaining  
155 subsections, we will describe more specific examples of how  
156 linkers are critical for the success of drug discovery programs and  
157 for the study of essential cellular processes.

158 **2.2. PROTAC Linker Considerations.** Proteolysis targeting  
159 chimeras or PROTACs represent a new method to target  
160 proteins of interest and degrade them to elicit a therapeutic  
161 response. This method exploits a chimeric molecule. A small  
162 molecule binder to an E3 ligase is linked to another small  
163 molecule that binds with the protein of interest. The targeted  
164 protein is then ubiquitinated after coming into close contact  
165 with the E3 ligase and degraded by the proteasome. One of the  
166 most critical decisions in designing a PROTAC is the length of  
167 the linker required to connect the small molecule binding to the  
168 protein of interest and the desired E3 ligase. PROTACs have  
169 been developed to degrade a variety of target proteins including

170 ALK,<sup>35</sup> the estrogen receptor,<sup>36</sup> MDM2,<sup>37,38</sup> tau,<sup>39</sup> BET protein,<sup>170</sup>  
171 and CDK9 protein. For these two last ones, the chimeric  
172 compounds JQ-1 and CDK9 are reported in Figure 3. Well- 172

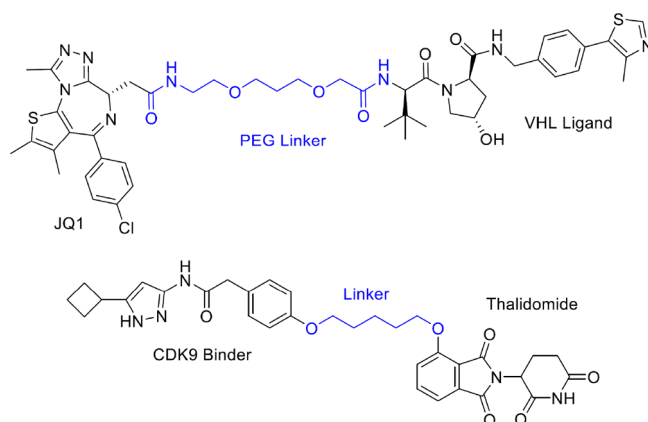


**Figure 3.** Chemical structures of the well-known, potent PROTACs including JQ1 and a CDK9 inhibitor, presenting the best linker length. Linkers are highlighted in blue.

173 established PROTACs are commercially available. After  
174 selection of which E3 ligase to target, typically either cereblon  
175 (CRBN) or von Hippel–Lindau (VHL), an appropriate linker  
176 between the E3 ligase binding moiety and the molecule binding  
177 the protein to be degraded needs to be installed.

178 An interesting study by the Kim group highlights how critical  
179 the linker length is in order to generate a potent degrader. They  
180 created an estrogen receptor (ER)- $\alpha$ -targeting PROTAC and  
181 installed a variety of linkers with different lengths. These linkers  
182 were composed of polyethylene glycol units, ranging in length  
183 from 11 to 16 atoms. Their results showed that while the 12- and  
184 16-atom linkers had similar binding affinities to the ER, the 16-  
185 atom linker was significantly more potent in degrading the ER.<sup>40</sup>

186 The importance of the linker length for a PROTAC was also  
187 demonstrated by the Krönke group.<sup>41</sup> They designed a homo-  
188 PROTAC for the degradation of the E3 ligase CRBN. If CRBN  
189 cannot ligate its cellular substrates, ubiquitinated proteins can  
190 increase, leading to cell death. They connected two thalidomide  
191 moieties with PEG linkers of various lengths and determined  
192 their abilities to degrade CRBN. In this case, the optimized  
193 linker was a short 8 atoms length PEG. These studies, along with  
194 many others, highlight that new PROTACs must be tested with  
195 a variety of different length linkers.<sup>42</sup> Linker dynamics, such as  
196 thermodynamics, linker flexibility, and decreasing steric clash,  
197 have been studied, and all of these parameters should be  
198 considered when designing a new PROTAC.<sup>43,44</sup>

199 **2.3. Linkers for the Discovery and Isolation of Natural**  
200 **Products.** Natural products represent a novel pool of potential  
201 antibiotic and anticancer molecules. Traditional purification  
202 techniques are biased toward discovering natural products that  
203 have been already identified. As described in the click chemistry  
204 section, it is a method to target alkyne-containing natural  
205 products, but these are a very small pool of natural products. The  
206 biggest challenge in discovering therapeutically relevant natural  
207 products is finding small molecules that have not been  
208 previously identified. Traditional extraction methods of a  
209 crude natural product lysate followed by LC/MS analysis is  
210 biased toward discovering the most abundant molecules in the  
211 lysate. Linkers that can isolate natural products based on their  
212 functional group composition have been developed. This 212

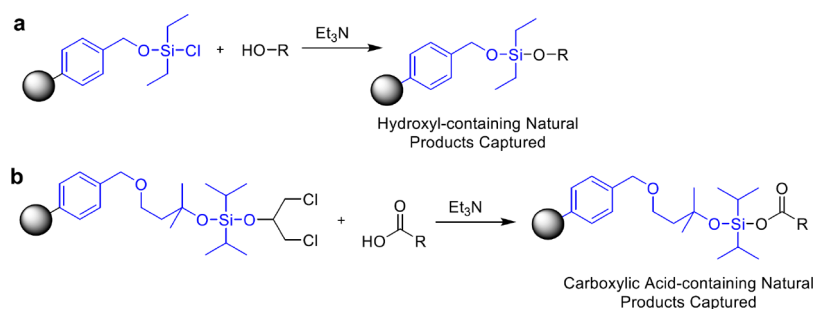


**Figure 4.** Linkers for the physical capture of natural products. Resins utilize a linker (colored in blue) with a silicon atom to capture (a) hydroxyl- or (b) carboxylic acid-containing molecules.

213 technique produces different pools of natural products, helping  
 214 to unmask those that are too low in abundance to be detected in  
 215 the crude lysate. The Carlson group has developed a family of  
 216 reversible linkers to isolate hydroxyl-, phenol-, and carboxylic  
 217 acid-containing natural products.<sup>45–48</sup> These linkers contain  
 218 different siloxy moieties that can selectively capture or release  
 219 different molecules containing the aforementioned functional  
 220 groups (Figure 4). The capture of hydroxyl-containing natural  
 221 products occurs by the formation of a silyl ether bond. This links  
 222 the natural product to the resin. Molecules not bound to the  
 223 resin are rinsed away using a variety of solvents. The molecules  
 224 linked to the resin can be released by exposing the resin to a  
 225 fluoride source, such as TBAF or HF. This creates two pools of  
 226 molecules, those that contain a hydroxyl moiety and those not  
 227 bearing this functional group. These unique pools of molecules  
 228 can be concentrated and analyzed by LC/MS or fractionated for  
 229 activity-based assays.

230 Linkers for the isolation of natural products containing other  
 231 functional groups have also been developed. There are several  
 232 examples of linkers to capture thiol containing natural products  
 233 through either a disulfide bond formation or a 1,4-nucleophilic  
 234 addition.<sup>49,50</sup> Linkers to natural products containing less  
 235 prevalent functional groups, including epoxides and  $\beta$ -lactams,  
 236 have also been described.<sup>51,52</sup>

#### 237 2.4. Linking Covalent Inhibitors to Fluorophores.

238 Monitoring and visualizing essential cell processes are critical  
 239 for drug development. The monitoring of enzymes critical to cell  
 240 survival is an important chemical biology technique. To  
 241 accomplish this, a number of covalent inhibitors have been  
 242 linked to fluorophores through a variety of linkers aiming to  
 243 visualize the desired cellular process. These probes can be used  
 244 in confocal microscopy and/or flow cytometry to evaluate the  
 245 effect of potential small molecule therapeutics. One example is  
 246 the development of a fluorescent derivative of Taxol (**2**) (Figure  
 247 5a). This cytotoxic drug was discovered ~50 years ago and has  
 248 been used to treat a variety of cancer types. **2** targets cells that  
 249 are rapidly dividing by interacting with microtubules and initiating  
 250 mitotic arrest. However, it is currently unclear the mechanism by  
 251 which **2** elicits its toxic effect and why some patients do not  
 252 respond to the treatment.<sup>53,54</sup> To visualize the subcellular  
 253 localization of **2**, the Peterson group synthesized a probe that  
 254 links this microtubule-stabilizing drug to Pacific Blue.<sup>55</sup> They  
 255 tested three different linker lengths between **2** and the Pacific  
 256 Blue moiety, and their results indicated that having a glycine  
 257 linker, rather than a  $\beta$ -alanine or GABA linker, led to the best  
 258 binding affinity to the tubulin heterodimer. Their probe was  
 259 highly specific for tubulin binding, and they proposed that it can  
 260 be used as a new tool for studying how **2** affects the proliferation  
 261 rate of cancer cells.

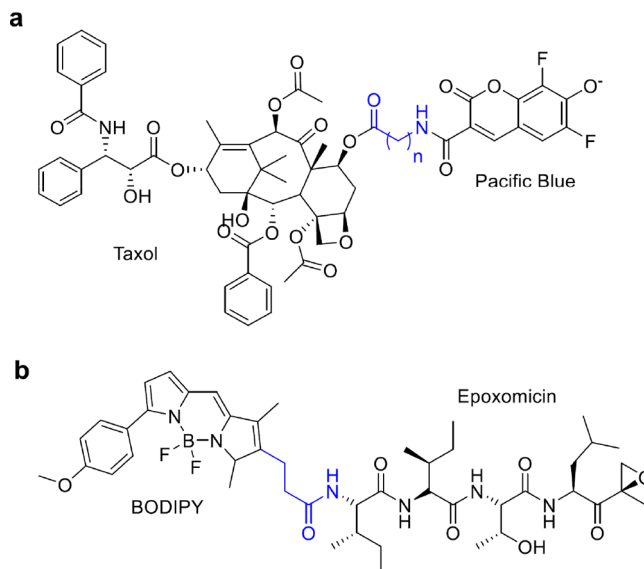


**Figure 5.** Two probes to observe (a) tubulin dynamics and (b) proteasome activity with the linker portion colored in blue. A variety of linker lengths between the small molecule binder/inhibitor and the fluorophore were evaluated to ensure that the fluorophore did not interfere with the binding to the protein of interest.

Fluorescent probes with a variety of linker types have also  
 262 been developed to monitor the activity of the proteasome. The  
 263 proteasome is a large protein complex in cells, responsible for  
 264 proteins degradation. If unwanted proteins accumulate in cells,  
 265 this can lead to endoplasmic reticulum stress and eventually  
 266 apoptosis.<sup>56–58</sup> Fluorescent probes have been developed to  
 267 study the activity of the proteasome in cells.<sup>59,60</sup> One of the  
 268 major considerations when developing a proteasome activity  
 269 probe is the linker length between the fluorophore and the  
 270 active-site binding moiety. The fluorophore must be far enough  
 271 from the binding site moiety to prevent any steric hindrance but  
 272 not too bulky that it cannot enter the catalytic channel of the  
 273 proteasome. The Overkleeft group has developed a number of  
 274 fluorescent probes to monitor the activity of the proteasome.  
 275 They have applied an activity probe that consists of the BODIPY  
 276 fluorophore linked to epoxomicin, a covalent inhibitor of the  
 277 proteasome (Figure 5b).<sup>61</sup> This probe, along with others with  
 278 different linker lengths, can be used to evaluate proteasome  
 279 activity and determine the composition of the different types of  
 280 active sites that assemble to form the full proteasome.<sup>62,63</sup> In  
 281 addition, a variety of probes with different types of linkers have  
 282 been developed to monitor the activity of the immunoprotea-  
 283 some.<sup>64</sup> The immunoproteasome rather than the standard 284

285 proteasome is produced when cells encounter an inflammatory  
286 signal.

287 The recent advancements in linker chemistry suggest that in  
288 the future linkers will allow making steps forward in the design of  
289 chimeras. Moreover, the linker will play a pivotal role in the  
290 delivery and release of therapeutic agents, as well as in the  
291 investigation of biological pathways.

### 3. CHIMERIC COMPOUNDS AND RECEPTOR-MEDIATED ENDOCYTOSIS

292  
293 **3.1. Receptor-Mediated Endocytosis for Drug Deliv-**  
294 **ery.** Lack of optimal pharmacokinetic profile is one of the main  
295 reasons why compounds fail during preclinical and clinical  
296 studies. Barrier permeability is an obstacle in achieving the  
297 therapeutic effect. Drug delivery opportunities are currently  
298 rising, and researchers are focusing their work on overcoming  
299 tissue barriers. Receptor-mediated endocytosis (RME, Figure 6)  
300 has been extensively studied as a method for boosting the  
301 transport of bioactive cargo across membranes, including the  
302 blood–brain barrier (BBB).

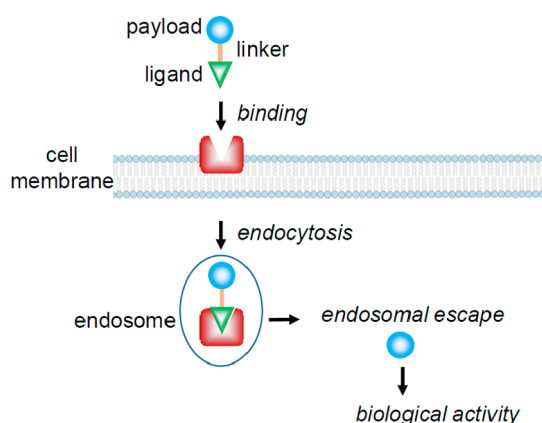


**Figure 6.** Schematic strategy of the selective delivery of biological cargo into cells exploiting receptor-mediated endocytosis.

303 Ligands binding to surface receptors can induce cellular  
304 uptake of therapeutics, including monoclonal antibodies,  
305 peptides, nucleic acids, small-molecule drugs, and nanoparticles.  
306 Herein, we discuss the recent advancements in the use of ligands  
307 for selectively binding to cell surface receptors. Three classes of  
308 ligands are discussed: (i) cell-penetrating peptides (CPPs), (ii)  
309 tumor homing peptides (THPs), and (iii) monoclonal antibodies.  
310 The highest ligand selectivity is displayed for antibodies, and  
311 this led to the FDA approval of five antibody–drug conjugates  
312 (ADCs): Mylotarg (3),<sup>65,66</sup> Besponsa (4),<sup>67</sup> Adcetris (5),<sup>68,69</sup>  
313 Kadcyla (6),<sup>70,71</sup> and Polivy (7).<sup>72</sup>

314 However, huge advancements have been shown also in the  
315 field of THPs. THPs are short peptides that have an inherent  
316 property to recognize tumor cells. Tumor necrosis factor  $\alpha$   
317 (hTNF $\alpha$ ) was conjugated with a tumor homing peptide  
318 (NGR),<sup>73,74</sup> and phase I and phase II clinical trials of NGR-  
319 hTNF $\alpha$  as a single agent and in combination with 1 are ongoing.  
320 In addition, THPs have a possible application in diagnostic  
321 imaging to help target radiopharmaceutical agents.<sup>75</sup> THPs  
322 represent a step forward in cancer diagnosis and treatment.

323 **3.2. Cell-Penetrating Peptides.** CPPs are considered the  
324 least selective ligands for RME and are believed to translocate  
325 across cell membranes via a receptor-independent mechanism.<sup>76</sup>  
326 Very recently, disclosures in cell-surface receptors responsible

for cellular uptake of CPPs paved the way for the optimization  
and exploitation of CPPs as ligands.<sup>77</sup>

327  
328  
329 CPPs are cationic and/or amphipathic peptides of typically  
330 8–30 amino acids and have been widely used to induce cellular  
331 uptake of bioactive cargoes.<sup>78–80</sup> CPPs can be either covalently  
332 or noncovalently be coupled with a cargo. Identification of key  
333 amino acids to induce cellular uptake has been a pivotal  
334 parameter for the development of efficient ligands. The isolation  
335 of the active transporting peptide sequence within the HIV-TAT  
336 (TAT48–57: GRKKRRQRRR) represented a breakthrough for  
337 CPPs development. This sequence is called TAT peptide or  
338 TAT.<sup>81</sup> Due to their high efficiency in internalization, arginine-  
339 rich CPPs such as oligoarginine and TAT facilitate the  
340 intracellular delivery of a wide range of cargoes, including  
341 peptides, antibodies, nucleic acids, nanoparticles, and small  
342 molecule drugs.<sup>82</sup> Different studies have reported the pivotal  
343 role of arginine as a basic amino acid in CPPs, since it interacts  
344 with the guanidinium and phosphate groups at the cellular  
345 membrane. Indeed, the surface of cancer cells is known to be  
346 more negative with respect to that of normal cells. The negative  
347 charge generated on cancer cells is related to the different sugar  
348 metabolism pathways from normal cells due to the higher  
349 amount of lactic acid production.<sup>83</sup> Positively charged CPPs  
350 bind through electrostatic interactions to the outside of cancer  
351 cells and promote RME.<sup>84</sup> However, the widespread use of  
352 CPPs is hampered by the lack of specific selectivity. TAT has  
353 been shown to strongly enhance the intracellular delivery of 1.  
354 Due to the nonspecific cell penetrating features of TAT, CPPs  
355 have been coupled to nanocarriers. Recently, Yang et al.  
356 developed acid-sensitive micelles as delivery method for TAT  
357 protection. The luteinizing hormone modified poly(ethylene  
358 glycol)-poly(L-histidine)-1 (LHRH-PEG-PHIS-1, Figure 7a)  
359 micelles were employed to deliver 1-TAT (Figure 7b). This  
360 strategy represents a step forward in the safer use of cytotoxic  
361 agents since the micelles dissociate in response to the tumor  
362 extracellular pH. Afterward, 1-TAT can cross the cell membrane  
363 of tumor cells and elicit a cytotoxic effect.<sup>85</sup>

364 In 2018, an anionic cell-penetrating tetrapeptide, Glu-Thr-  
365 Trp-Trp (ETWW), with excellent potential for cell penetration,  
366 has been reported. The tetrapeptide has been coupled to  
367 liposomes to efficiently deliver 1 to the nucleus of cancer cells.<sup>86</sup>  
368 Very recently, Dominguez-Berrocal et al. developed a chimeric  
369 trifunctional peptide composed of a CPP, a nuclear localization  
370 sequence, and a peptide blocking the interaction of the primary  
371 downstream effectors of the Hippo signaling pathway (TEAD  
372 and YAP). The novel peptide delivered the cargo specifically to  
373 the nucleus and showed an apoptotic effect in tumor cell lines.  
374 The antitumor efficacy in a breast cancer xenograft model is  
375 encouraging for the development of nuclear anticancer drugs.<sup>87</sup>

376 In addition to cancer treatment, nanoparticle-forming CPPs  
377 have been investigated in gene therapy approaches. However,  
378 CPP-mediated plasmid DNA (pDNA) delivery has been  
379 inefficient mostly because CPPs condense pDNA into nano-  
380 particles that easily disintegrate, without delivering the  
381 therapeutic amount of pDNA into cells. In addition, CPPs and  
382 their cargo could be trapped into endocytic vesicles, preventing  
383 the pDNA from reaching the nucleus. These limitations can be  
384 overcome with the addition of a hydrophobic stearic acid residue  
385 since hydrophobic interactions are essential to form and stabilize  
386 the CPP/pDNA nanoparticles. Veiman et al. proposed  
387 pepFect14 (stearyl-AGYLLGKLLLOOLAAAALLOOLL, PF14,  
388 where O is ornithine) as a suitable non-natural peptide to  
389 form stable nanoparticles with pDNA. These nanoparticles 389

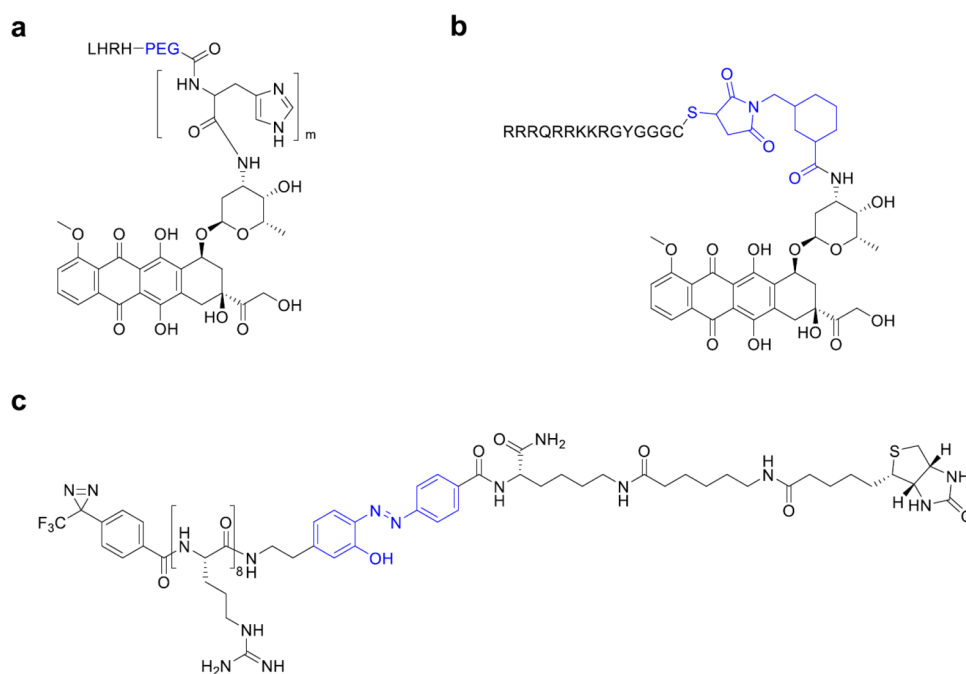


**Figure 7.** (a) LHRH-PEG-PHIS-1. (b) 1-TAT conjugate. (c) Cleavable probe of octa-arginine peptide. Linker is colored in blue.

could lead to an efficient gene delivery allowing the optimal transfection of genetic material into cells.<sup>88</sup> The uptake of PF14 and other CPP/oligonucleotide (siRNA or pDNA) complexes is mediated by scavenger receptors (SCARA).<sup>89</sup> These receptors bind promiscuously all negatively charged macromolecules and mediate their uptake.<sup>90</sup>

Another noteworthy application of CPPs is the delivery of neuroprotective peptides to the central nervous system for the treatment of neurological disorders. Arginine-rich CPPs show promising results in the delivery of neuroprotective peptides, especially to aid in treating cerebral ischemia and stroke. Several groups have shown that TAT and other arginine-rich cell penetrating peptides have intrinsic neuroprotective properties.<sup>91,92</sup> Meloni et al. suggested that the neuroprotection might be related to carrier peptide endocytosis: neuronal cell surface structures such as ion channels and transporters are internalized during endocytosis, decreasing the calcium influx associated with excitotoxicity.<sup>93</sup> In addition, endocytosis causes internalization of cell surface receptors leading to a decrease in receptor-mediated neurodamaging signaling pathways.<sup>94</sup>

Endocytosis has a crucial role in the cellular uptake of CPPs. Macropinocytosis<sup>95</sup> and other classes of endocytosis such as clathrin-mediated<sup>96</sup> and caveolae-mediated endocytosis<sup>97</sup> are involved. Moreover, direct penetration of CPPs through plasma membranes has been described.<sup>98</sup> Originally it was believed that CPPs translocated across cell membranes via a receptor-independent mechanism, leading to a not-cell-type-specific uptake.<sup>76</sup> Very recently, Kawaguchi et al. identified syndecan-4 as a cell-surface receptor responsible for cellular uptake of octa-arginine (R8) peptide via clathrin-mediated endocytosis. A cleavable probe of the R8 peptide (Figure 7c) was used to identify syndecan-4 as an endogenous membrane-associated receptor.<sup>77</sup> Even though this cell-surface receptor is ubiquitously expressed, it is overexpressed in breast and testicular cancer cells<sup>99,100</sup> and in kidney cells of patients with IgA nephropathy.<sup>101</sup>

Rodríguez Plaza et al. proposed that CPPs work as cationic antibacterial peptides (CAPs) in the presence of bacterial cells. While CPPs enter eukaryotic cells without apparent toxicity, CAPs are able to make pores in the membrane and kill bacteria. Iztli peptide 1 (IP-1), showing both CPP and CAP activities, was utilized to explain this different behavior. IP-1, a hunter–killer peptide against *Saccharomyces cerevisiae*, makes pores only in the presence of high electric potential value at the membrane, which have been found in bacteria and mitochondria.<sup>102</sup> Therefore, CPPs are able to switch from penetrating mammalian cells with any apparent toxicity to killing bacterial cells in the presence of large membrane potential.<sup>102,103</sup>

**3.3. Tumor Homing Peptides.** As described in section 3.2, the majority of CPPs lack specificity leading to reduced therapeutic efficiency and side effects. To overcome the limitations of CPPs, more specific peptides, namely, tumor homing peptides (THPs), have been developed.<sup>104</sup> THPs are short peptides constituted by a few amino acids (3–15) and are considered a type of CPP. They have the intrinsic property to recognize oncological-specific proteins and molecular markers overexpressed on tumor cells or tumor vasculature.<sup>105</sup> After binding to cell surface receptors, tumor homing peptides induce RME. Classical vascular-homing peptides are peptides containing the NGR motif, which binds to aminopeptidase N (CD13) or the RGD motif, which binds to  $\alpha_v$  integrins.<sup>106</sup> Aminopeptidase N is overexpressed by endothelial cells of tumor vasculature and has been demonstrated to be involved in angiogenesis and cancer progression. Likewise,  $\alpha_v$  integrins are overexpressed in blood vessels in the tumor and represent a potential target to deliver cytokines to tumor vasculature. **1** was the first anticancer drug to be coupled to a NGR peptide. Later, phase I and phase II clinical trials of NGR-hTNF $\alpha$  as a single antitumor agent and in combination with **1** have been performed for a variety of cancers, including ovarian, colorectal, and small cell lung cancer (SCLC).<sup>107,108</sup> Tumor necrosis factor  $\alpha$  (TNF $\alpha$ ) has demonstrated powerful antitumor activity but also severe toxicity. Conjugation of hTNF $\alpha$  with the tumor

463 homing peptide NGR (Figure 8) improved safety and efficacy of  
464 TNF. Moreover, a synergism between NGR-hTNF $\alpha$  and

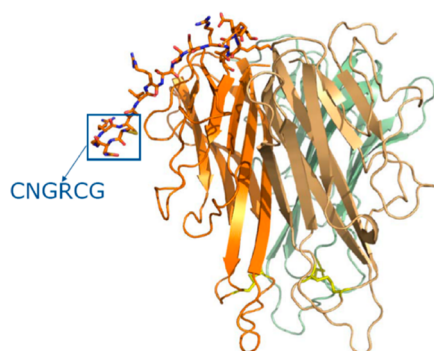


Figure 8. Structure of a monomer NGR-hTNF [<https://www.molmed.com/node/33>].

465 chemotherapy was observed, since NGR-hTNF $\alpha$  has been  
466 shown to increase the intratumoral chemotherapy penetra-  
467 tion.<sup>73</sup> Very recently, phase II clinical results have been disclosed  
468 and NGR-hTNF plus 1 demonstrated promising activity in  
469 patients with relapsed SCLC.<sup>74</sup> A phase III clinical trial was  
470 performed in patients with malignant pleural mesothelioma to  
471 assess the efficacy and safety of NGR-hTNF plus best  
472 investigator choice [NCT01098266]. Despite the positive  
473 results in phase II evaluation, the phase III clinical trial did  
474 not meet its end point; no significant differences in overall  
475 survival were observed between treated groups. However,  
476 further investigation is needed due to the poor prognosis of  
477 patients after first-line treatment.<sup>109</sup>

478 In addition to the TNF protein, the TNF gene has been  
479 employed for cancer gene therapy and has been reported to  
480 promote antitumor responses both in animal models and in  
481 patients. The plasmid DNA encoding CNGRCG-TNF and  
482 ACDCRGDCFCG-TNF (pNGR-TNF and pRGD-TNF, re-  
483 spectively) displayed growth inhibition of subcutaneous murine  
484 B16F1 melanomas and RMA-T lymphomas after intramuscular  
485 injection.<sup>110</sup> RGD-TNF $\alpha$  was also evaluated for its ability to  
486 enhance the antitumor effect of chemotherapy; however NGR-  
487 hTNF $\alpha$  was mostly chosen for clinical trials. RGD has been  
488 preferentially exploited for diagnostic applications and many  
489 RGD-based radiopharmaceutical agents have been assessed for  
490 cancer imaging.<sup>75</sup> Bispecific NGR peptides (GNGRAHA),  
491 targeting both CD13 and  $\alpha v \beta 3$  integrin in the endothelium of  
492 solid tumors, have been developed. In 2018, Seidi et al.  
493 combined the NGR peptide, GNGRAHA, with a truncated form  
494 of coagulase (tCoa) generating a bifunctional protein (tCoa-  
495 NGR) with novel anticancer properties. This strategy allowed  
496 selective targeting of the tumor neovasculature and inducing of  
497 selective thrombosis in tumor-feeding vessels. In tumor models,  
498 tCoa-NGR led to a significant reduction of tumor growth after  
499 systemic administration.<sup>111</sup> Therefore, tCoa-NGR represents a  
500 promising anticancer strategy to induce tumor infarction and  
501 reduce systemic side effects.

502 Besides TNF, tumor homing peptides could facilitate  
503 distribution of other cytokines into tumor cells and enhance  
504 their therapeutic effect. In 2017, it has been shown that RGD  
505 enhances the antitumor effect of IL-24. Melanoma differ-  
506 entiation-associated gene-7/interleukin-24 gene (MDA-7/IL-  
507 24) is a unique tumor suppressor gene, which promotes selective  
508 apoptosis of cancer cells. RGD-coupled IL-24 construct induced

apoptosis in hepatocellular carcinoma-related cell line.<sup>112</sup> The  
510 results highlight the benefit of cytokine targeting by THPs to  
511 cancer cells. Coupling RGD to the N-terminus of IL-24 led to a  
512 stronger interaction with the receptors. On the contrary, adding  
513 RGD to the C-terminus of IL-24 disrupted native interactions  
514 and reduced the apoptosis induction properties.<sup>113</sup> Very  
515 recently, Bina et al. confirmed these results with *in silico*  
516 targeting of RGD/NGR-modified IL-24 to tumor cells.<sup>114</sup>

517 THPs have shown potential to be versatile platforms of  
518 polymers for nonviral gene delivery.<sup>115</sup> pDNA complexes of  
519 recombinant proteins with poly(L-lysine) and THP showed  
520 significant improvement of target specificity to cancer cells by  
521 additions of F3 and CGKRK THPs. F3 peptides are high affinity  
522 ligands for nucleolin, which is expressed on the surface of cancer  
523 angiogenic endothelial cells, and selectively bind MDA-MB-435  
524 cells.<sup>116,117</sup> CGKRK peptides were described to bind to heparin  
525 sulfate in cancer vessels.<sup>118,119</sup>

526 THP-gold nanoconjugates actively targeted MCF-7 cells in  
527 comparison to nontumor 3T3-L1 fibroblast cells.<sup>120</sup> THPs  
528 specific for MCF-7 cells were selected from a phage display  
529 library, synthesized, and conjugated to spherical gold nano-  
530 particles by a heterobifunctional cross-linker with an ethylene  
531 oxide spacer. This work proved the possibility of developing  
532 nanomaterials that can rely on tumor targeting potential  
533 irrespective of a specific knowledge of the target cell biology.

534 **3.4. Monoclonal Antibodies.** Over the past decade,  
535 monoclonal antibodies (mAbs) have significantly improved  
536 the clinical outcomes for cancer patients since they specifically  
537 bind tumor-associated target antigens and eventually deliver  
538 cytotoxic agents to tumor cells in a targeted manner while  
539 sparing normal cells.<sup>121</sup> mAbs are conjugated to small-molecule  
540 chemotherapeutics, and the resulting antibody-drug conjugate  
541 (ADC) is parentally administered (intravenous or subcuta-  
542 neous). After binding to their target antigens, ADCs are  
543 internalized through RME.<sup>122</sup> The development of a procedure  
544 to produce mAbs has increased the enthusiasm of scientists for  
545 the development of precise targeted cancer therapy. Humanized  
546 and fully human antibodies have the advantage of being retained  
547 longer in circulation than their murine equivalents and led to a  
548 dramatic increase in the use of antibody-based drugs against  
549 cancer.<sup>123,124</sup> However, many challenges have to be overcome  
550 for the development of optimized and functional antibody-drug  
551 conjugates with possible application as therapeutic agents.

552 One of the major challenges in the development of ADCs is to  
553 incorporate a linker able to preserve the ADC stability in  
554 systemic circulation for an extended period and to release the  
555 payload at the targeted site. Conjugation site and linker choice  
556 are key parameters in the pharmacokinetic properties of ADCs.  
557 The site of attachment to an antibody can also be engineered in  
558 different ways to incorporate a linker and subsequently a  
559 bioactive molecule.

560 Considering the five ADCs approved so far by FDA, 560  
561 gemtuzumab ozogamicin (3) and inotuzumab ozogamicin (4)  
562 have an acid-sensitive hydrazone linker (Figure 9), brentuximab  
563 vedotin (5) and polatuzumab vedotin (7) have a lysosomal  
564 protease-sensitive peptide linker (Figure 10a), and trastuzumab  
565 emtansine (6) exploits a noncleavable SMCC (*N*-succinimidyl-  
566 4-(maleimidomethyl)cyclohexane-1-carboxylate) linker (Figure  
567 10b).

568 Compound 3 uses side chain reactive lysines of a humanized  
569 anti-CD33 mAb to attach calicheamicin, a highly cytotoxic agent  
570 that induces double-strand DNA cleavage, by a bifunctional acid  
571 sensitive hydrazone linker (Figure 9). After being launched in

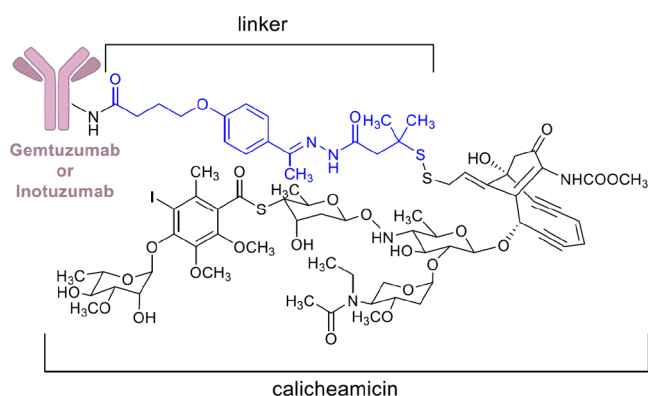


**Figure 9.** Chemical structure of **3** and **4**. Linker is colored in blue.

2000 as therapeutic agent for relapsed acute myelogenous leukemia, this ADC was withdrawn from the market due to the limited benefit over conventional anticancer treatment and the serious hepatotoxicity.<sup>125,126</sup> This withdrawal increased the concern on the stability of the hydrazone linker. In addition, the ADC heterogeneous nature of the drug conjugate concurred to premature release of the conjugated payload, leading to a significant toxicity compared to traditional chemotherapy. Subsequent trials using a lower dose led, in September 2017, to the FDA approval of **3** for newly diagnosed and relapsed/refractory acute myeloid leukemia.<sup>65,66</sup>

Compound **4** is another antibody–drug conjugate of calicheamicin.<sup>127</sup> It is formed by a CD22-directed monoclonal antibody covalently bonded to *N*-acetyl- $\gamma$ -calicheamicin (Figure 9). **4** received FDA approval in 2017 to treat relapsed or refractory CD22-positive B-cell precursor acute lymphoblastic leukemia.<sup>67</sup> **4** has shown excellent activity in the clinic, and ongoing trials are evaluating its value as frontline treatment.<sup>128</sup> A

phase III clinical trials is assessing the benefits of treating newly diagnosed B-cell acute lymphoblastic leukemia with **4** in combination with chemotherapy [NCT03150693].

In 2011, compound **5** received approval for Hodgkin's lymphoma (HL) and anaplastic large-cell lymphoma (ALCL).<sup>68,69</sup> **5** utilizes side chain cysteines to conjugate monomethyl auristatin E (MMAE), a potent antimitotic agent, with the anti-CD30 mAb (cAC10) through an enzymatically cleavable dipeptide (valine–citrulline) linker (Figure 10a).<sup>129</sup> A selective reduction of the disulfide bonds in the four interchain provides up to eight reactive sulfhydryl groups that facilitate drug conjugation (drug to antibody ratios are from 0 to 8).<sup>130,131</sup> Exploiting this method to link the drug, rather than using lysine conjugation, results in ADCs that could be easily purified and pharmacokinetically characterized. Besides its application in the treatment of different types of lymphomas, the safety and antitumor activity of **5** have been demonstrated also in patients with CD30-expressing solid tumors in a phase II clinical trial.<sup>132</sup>

In 2019, compound **7**, a second ADC of MMAE whose mAb targets CD79b (B-cell antigen receptor complex-associated protein  $\beta$  chain), was granted accelerated FDA approval for the treatment of adults with relapsed or refractory diffuse large B-cell lymphoma (DLBCL) in combination with bendamustine plus rituximab (BR).<sup>72</sup> A multicenter phase Ib/II clinical trial including a cohort of 80 patients with relapsed or refractory DLBCL [NCT02257567] granted drug approval. At the end of the therapy, the complete response rate was 40% with **7** plus BR, compared with 18% with BR alone.<sup>133</sup>

Compound **6** uses a noncleavable SMCC linker to cross-link the warhead cytotoxic agent emtansine (DM1), a microtubule inhibitor, to lysine residues of anti-HER2 mAb, trastuzumab (Figure 10b). Lysine-MCC-DM1 complex, an intercellular metabolite, turned out to be as active as the parent drug, after

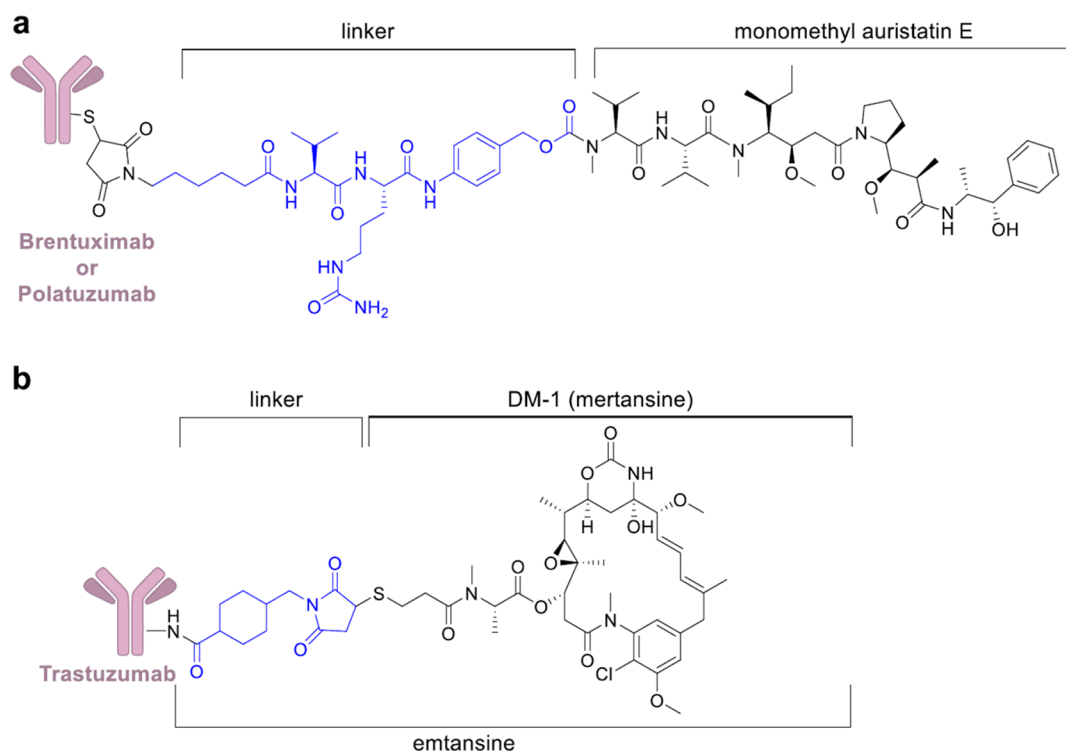


**Figure 10.** (a) Chemical structure of **5** and **7**. (b) Chemical structure of **6**. Linkers are colored in blue.

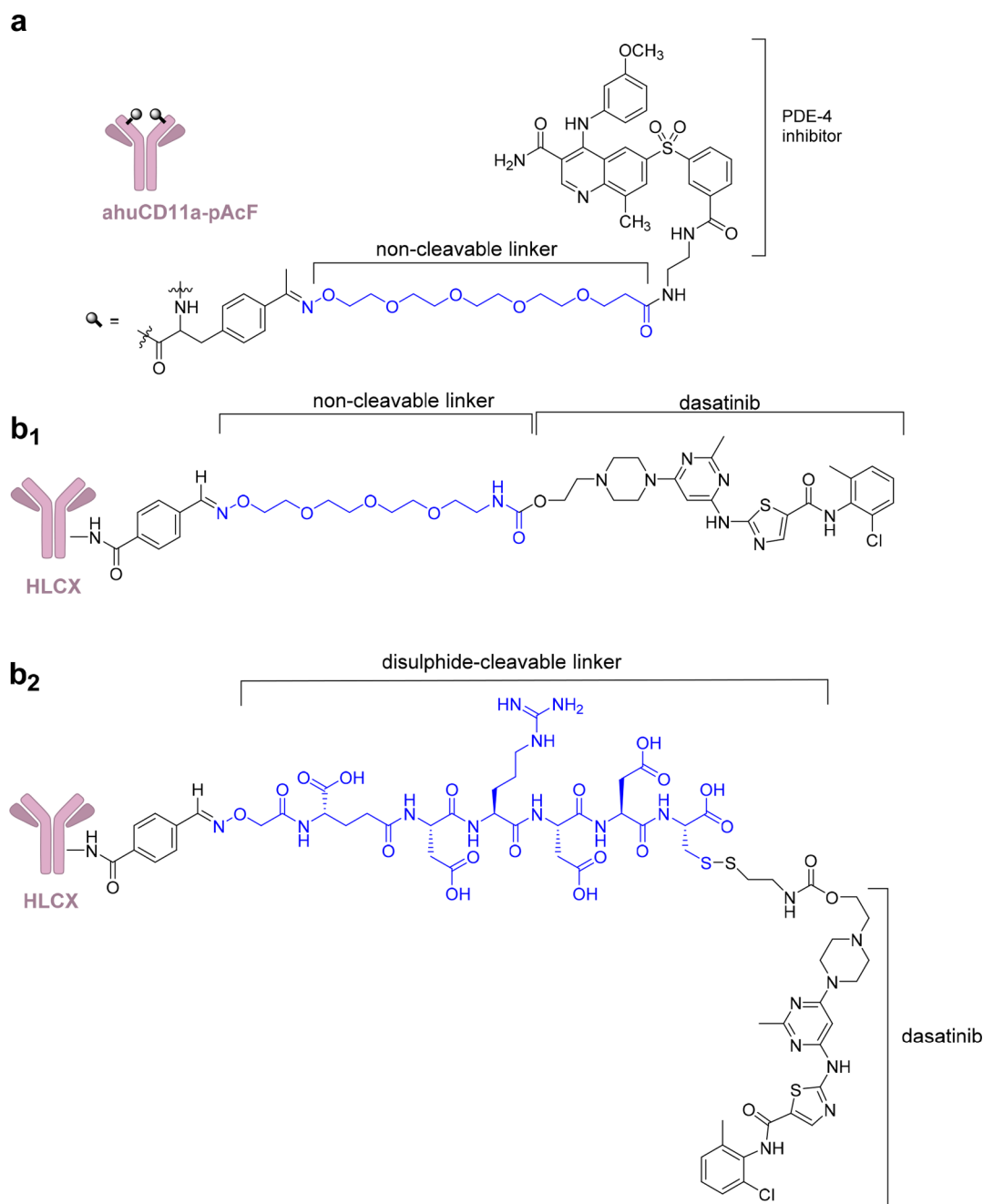


**Figure 11.** (a) Anti-inflammatory human  $\alpha$ CD11a antibody conjugated to a PDE4 inhibitor. (b<sub>1</sub>, b<sub>2</sub>) HLCX, immunosuppressive humanized antibody that binds selectively to CXCR4, conjugated to 8 with a noncleavable linker (b<sub>1</sub>) and a disulfide-cleavable linker (b<sub>2</sub>). Linkers are colored in blue.

624 trastuzumab degradation by lysosomes. It is clinically employed  
 625 in patients with HER2-positive metastatic breast cancer.<sup>70,71</sup>

626 The approval of 6 for the treatment of breast cancer highlighted  
 627 the capability of ADCs to target solid malignancies in addition to  
 628 hematologic tumors. With the recent approval of 7, there has  
 629 been a boost in research investigating the use of ADCs in cancer  
 630 treatment. ADCs are likely to become a pivotal part of future  
 631 targeted cancer therapy.

632 Although a huge effort has been made to produce ADCs for  
 633 oncology, they are also an attractive platform to deliver  
 634 nontoxic bioactive cargos in a cell-specific way aiming to  
 635 reduce potential side effects related to off-target interactions. For  
 636 example, an antibody–drug conjugate that selectively recognizes  
 637 immune cells through the CD11a antigen has been conjugated

to a derivative of a highly potent phosphodiesterase 4 (PDE4)  
 inhibitor (GSK256066) (Figure 11a). This strategy could limit  
 neurological side and gastrointestinal toxicity that have  
 hampered a broad application of PDE4 inhibitors.<sup>134</sup> To obtain  
 a site-specific conjugation to the anti-human CD11a antibody,  
 the unnatural residue *p*-acetylphenylalanine (pAcF) was linked  
 to the heavy chain of efalizumab (site A122). To enable  
 conjugation of GSK256066, a linker containing a tetraethylene  
 glycol spacer with a terminal amino group was reacted under  
 slightly acidic conditions with the pAcF ketone, resulting in  
 stable covalent conjugates. Conjugation was performed with  
 drug/antibody ratio of 2 (1 bioactive molecule linked to each  
 heavy chain). Recent studies have supported the feasibility to  
 develop mAbs–PDE4 inhibitor conjugates as promising

652 therapeutics for treating ulcerative colitis due to the specific  
653 delivery of immune suppressants to immune compartment.<sup>135</sup>  
654 In addition, autoimmune diseases represent a potential field for  
655 ADCs application and significant advancements have been done  
656 in the past decade. Wang et al. proposed the use of dasatinib (**8**),  
657 a Bcr-Ab1 tyrosine kinase inhibitor, for immune suppression and  
658 developed an immunosuppressive ADC (Figure 11b) which  
659 targets CXCR4 and delivers **8** to human T lymphocytes.  
660 Modeling and structure–activity relationship studies high-  
661 lighted that the hydroxyl moiety of **8** is not required to observed  
662 pharmacological activity.<sup>89,90</sup> Therefore, it was modified for  
663 conjugation to the antibody with a noncleavable linker by  
664 reaction with *p*-nitrophenyl chloroformate and carbamylation  
665 with a tetrapolyethylene glycol (PEG) linker displaying an  
666 aminoxy group. The resulting **8**–antibody conjugate inhibits T  
667 cell receptor (TCR)-mediated T cell activation and cytokine  
668 expression with nanomolar EC<sub>50</sub> and shows minimal effects on  
669 cell viability. This strategy could lead to an improved efficacy  
670 and safety of kinase inhibitors and to their exploitation in  
671 nononcological diseases.<sup>136</sup> A phase II clinical trial is currently  
672 ongoing to determine the benefit of **5** in the treatment of  
673 systemic sclerosis, a multisystem autoimmune disease  
674 [NCT03198689].

675 These results highlight that, besides cancer, ADCs have  
676 potential application in a wide range of inflammatory and  
677 autoimmune disorders. Naked therapeutic antibodies have  
678 launched a novel era of both autoimmune disease and cancer  
679 treatment, but ADCs represent the next-generation antibody  
680 therapies and will represent a breakthrough in the treatment of  
681 these illnesses.

682 The ability of monoclonal antibodies to selectively bind  
683 tumor-associated target antigens and release cytotoxic agents to  
684 the tumors in a targeted manner has dramatically improved the  
685 clinical practice. Further advancements in this field will lead to  
686 the success of precise targeted cancer therapy. RME is also  
687 exploited by CPPs and THPs, but they have a poor selectivity  
688 compared to antibodies. However, nanocarriers are attractive  
689 tools to be coupled to CPPs and THPs and improve their safety  
690 and selectivity. In addition, the use of nanocarrier is boosting the  
691 antibody-based delivery of biological cargos into cancer cells. In  
692 the future, these systems are expected to become essential  
693 therapeutics for the treatment of malignancies and central  
694 nervous system disorders. Moreover, THPs are essential  
695 components of radiopharmaceutical agents and will represent  
696 a step forward in cancer diagnosis.

#### 697 4. CHIMERIC COMPOUNDS AND TARGET 698 ENGAGEMENT

699 **4.1. Target Engagement.** One of the main failures in  
700 translating preclinical results into a positive clinical outcome is  
701 the lack of pharmacokinetic and pharmacodynamic validation of  
702 drug–target interactions *in vivo* with serious impact on efficiency  
703 and costs of the drug discovery process. The mechanism that  
704 small molecules adopt to engage their targets inside living cells is  
705 a crucial step in medicinal chemistry and chemical biology, since  
706 it requires the availability of appropriate assays and inhibitors/  
707 ligands. The molecular recognition event in living cells between  
708 drugs and targets is defined as “target engagement”, and the  
709 associated technologies represent a rapidly evolving field of  
710 research.<sup>137–140</sup>

710 This technology allows target validation in living systems: in  
711 cells, tissues, and animal models. It confirms compounds cellular  
712 entry and target binding and can suggest optimized drug delivery

to enable compounds to be more effective, specific, bioavailable,  
713 and less toxic.<sup>2,141,142</sup> *In vitro* studies could foresee the  
714 optimization of human performance characteristics.<sup>143</sup> To  
715 perform these studies, selected leads and drugs should be  
716 conjugated with appropriate tags to obtain chimeric compounds  
717 with a diversity of structures (see Figure 1).<sup>2,141,142</sup>

718 To perform a target engagement study, it is essential to (i)  
719 know the target localization into the cell, (ii) design an assay for  
720 cellular setting, (iii) ensure the detection of the observable  
721 changes on cellular surface or intracellularly, depending on  
722 targets location, and (iv) ensure the escape of off-targets and  
723 background noise of the cellular matrices.<sup>144</sup> While quantifica-  
724 tion of compound binding to purified proteins or surface  
725 receptors (in particular to GPCR) is well established,<sup>145,146</sup>  
726 the interaction of compounds with intracellular targets is difficult to  
727 quantify.

728 Regarding the fluorimetric detection, a fluorescent probe has  
729 to be covalently conjugated with the inhibitor (see section  
730 2.4)<sup>2,141,142</sup> and should show sufficient solubility (slightly  
731 different from the values required for a drug) and a log *P*  
732 of around 3, necessary for a suitable drug or inhibitor tagging.  
733 Lipophilicity may influence the amount of compound able to  
734 enter the cell and consequently available for binding. In addition,  
735 the fluorescent tag module should not mask the compound  
736 affinity for the target (see section 2). Target engagement assays  
737 might be invasive since they drive the intracellular environment  
738 away from equilibrium conditions.<sup>147–149</sup> Orthogonal assays are  
739 usually needed to validate the results.<sup>150</sup> Atkinson and co-  
740 workers studied the interaction of selective autophagy receptors  
741 with two conserved hydrophobic pockets (called W-site and L-  
742 site) of mATG8 (autophagy receptors to autophagy related 8)  
743 proteins through a linear residue, namely, the LC3-interacting  
744 region (LIR). Fourteen LIR-containing peptides were designed  
745 and synthesized, and their affinity for mATG8 was investigated  
746 using a competitive time-resolved FRET (TR-FRET). The assay  
747 used a GST-tagged mATG8 protein and a terbium labeled anti-  
748 GST antibody to measure the equilibrium dissociation constant,  
749 *K<sub>d</sub>*, by TR-FRET. The results were confirmed by additional  
750 structural information using nuclear magnetic resonance  
751 (NMR) spectroscopy. This work points out the importance of  
752 having two assays that exploit different experimental readouts to  
753 validate the results.<sup>150</sup>

754 A similar approach was reported to discover inhibitors of the  
755 signal-regulatory protein (SIRP) $\alpha$ -CD47 interaction with a  
756 high-throughput screening approach.<sup>151</sup> CD47 is an immune  
757 checkpoint that downregulates the functionality of both innate  
758 and adaptive anticancer immune response through its SIRP $\alpha$   
759 receptor. A series of small molecule ligands that selectively target  
760 SIRP $\alpha$  interactions with CD47 was discovered. The assay was  
761 performed using a specific LANCE TR-FRET assay and a  
762 ~90 000-compound library. In parallel, an AlphaScreen based  
763 on similar TR-FRET technology was adopted for validation  
764 purposes. SIRP $\alpha$  was biotin tagged, and an antibody with the  
765 energy donor reagent was the tagged chimeric biomolecule  
766 exploited in the assays.

767 In the following subsections, target engagement technologies  
768 and examples of the use of tagged compounds are described.

769 **4.2. Strategies Based on Small Molecule and Target  
770 Protein Modification.** The proximity between a bioactive  
771 small molecule and its targeted protein can be studied using  
772 spectroscopic methods such as fluorescence or bioluminescence  
773 resonance energy transfer measurements (FRET and BRET,  
774 respectively). FRET and BRET occur only when the donor and  
775

776 acceptor are in close proximity (2–6 nm) and are unique  
777 methods to inspect intermolecular protein interactions and  
778 protein–ligand interactions in cells.<sup>152</sup>

779 In FRET (fluorescence resonance energy transfer or Förster  
780 resonance energy transfer) studies, a donor fluorophore upon  
781 excitation transfers energy to a nearby acceptor fluorophore.  
782 When a suitable acceptor is present, the donor emission is  
783 quenched and emission of light occurs at a longer wavelength  
784 (Figure 12). The essential criteria to observe FRET are (i)

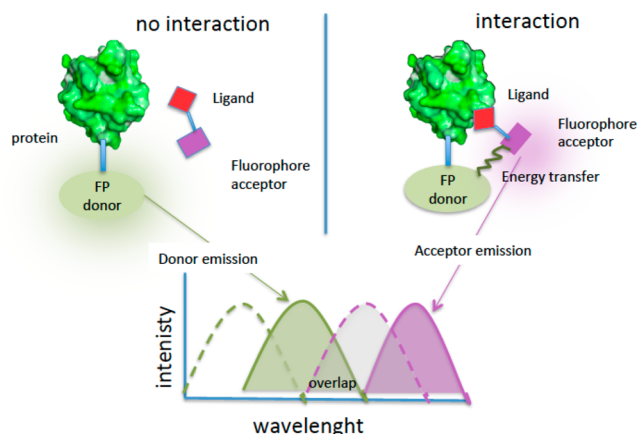


**Figure 12.** Description of FRET experiments for target engagement with no interaction (left) and interaction (right): FP, fluorescent protein; green dot line = donor excitation spectrum; green line = donor emission spectrum; violet dot line = acceptor excitation spectrum; violet line = acceptor emission spectrum.

785 suitable distance, (ii) appropriate donor/acceptor orientation,  
786 and (iii) large overlap of the donor emission spectrum and the  
787 acceptor absorption spectrum. FRET can be quantified  
788 determining the change in donor fluorescence lifetime through  
789 fluorescence lifetime imaging microscopy (FLIM) based on  
790 FRET readout.<sup>153–155</sup> FRET-FLIM monitors target engage-  
791 ment in living cells and provides details on the temporal and  
792 spatial distribution of the ligand–protein complex.

In some cases, a fluorescent protein (FP) is fused in cells to  
the target protein, and a FRET signal is generated when  
fluorophores are in close proximity (Figure 12, left). In a  
different protocol, the target protein can be ectopically  
expressed in the same cells and modified in a specific residue  
in order to bind a suitable fluorescent donor (or acceptor)  
(Figure 12, right).<sup>156,157</sup> The target protein could be properly  
engineered to allow binding detection, for example, with a  
tetracysteine tag.<sup>156,157</sup> Cells expressing the target protein  
coupled to a FP are treated with the a small molecule labeled  
with a fluorescent dye; subsequently the lifetime distribution of  
the donor fluorophore into a cell is determined. The donor  
fluorescence lifetime reveals the interaction sites into a cell  
as well as the areas with a reduced donor lifetime.

FRET based technology has been exploited, for example, for  
the recognition of phosphodiesterase<sup>158</sup> and thymidylate  
synthase (TS) by tagged inhibitors. TS is an obligate  
homodimeric enzyme, and a tetracysteine (TC4) tag is  
introduced at the N-terminus. The fluorescein diarsenical  
probe FAsH, added to the HEK-293 cell lysate containing the  
ectopically expressed protein, is coordinated by the tetracysteine  
behaving as a fluorescence donor. The tagged substrate is an  
octapeptide (LR) and is conjugated with the fluorescence  
acceptor probe Hylite-405 (Figure 13). Titration of hTS  
tetracyc-Flash (acceptor) with LR-hylite 405 (donor) in lysates  
of cells transfected with hTS-tetracyc shows an increase in FRET  
signal.

TR-FRET has been applied to the assessment of Bruton's  
tyrosine kinase (BTK) occupancy in the clinical trials of  
tirabrutinib (9). Compound 9 (GS-4059/ONO-4059) is a  
second-generation, irreversible BTK inhibitor explored for the  
treatment of lymphoid malignancies. The inhibitor was  
conjugated with biotin through a carbamide–PEG mixed linker,  
and free and total BTK levels were measured using TR-FRET.<sup>154</sup>

**4.3. BRET Experiments.** BRET (bioluminescence resonance energy transfer) is a mechanism describing the energy transfer between a donor (luciferase) and an acceptor (fluorescent) molecule. The spectral separation between donor and acceptor excitation required in FRET (Figure 13)

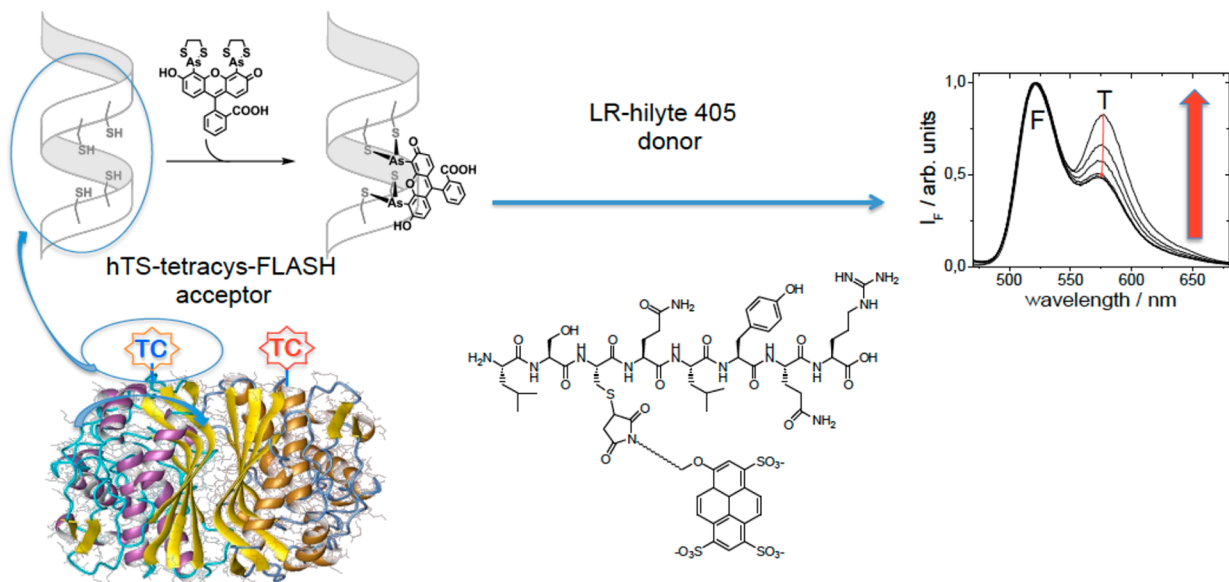


**Figure 13.** FRET experiment with TS dimer. The N-terminus is modified by inserting the sequence CCGPCC-tetracysteine (TC). Probe excitation at the proper wavelength causes the energy transfer and FRET signal increases upon binding of the LR-hylite-405 ligand.

is not required in BRET since the production of light originates from a chemical reaction catalyzed by the donor enzyme (Figure 14, right). Since BRET does not require the use of excitation

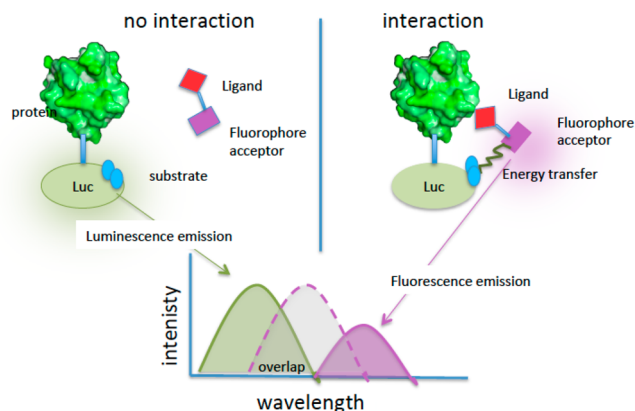


**Figure 14.** Description of BRET experiments for target engagement with no interaction (left) and interaction (right): Luc, luciferase; green line = donor emission spectrum; violet dot line = acceptor excitation spectrum; violet line = acceptor emission spectrum.

illumination, it has advantages over FRET. BRET is therefore more applicable to the analysis of photoresponsive cells or cells that are easily damaged by excitation light. BRET has been exploited to detect protein–protein interactions in real time in living cells.<sup>159,160</sup> In target engagement studies, cells express the target protein fused to a luciferase, while a ligand with a fluorophore tag behaves as an acceptor (Figure 14). Different BRET techniques are known and differ for the combination of the donor/acceptor/substrate used.<sup>161</sup> Distance, orientation, and spectral overlap are the major parameters that influence both BRET and FRET. However, external excitation of the donor is not required in BRET; therefore phenomena related to simultaneous donor/acceptor excitation, fluorescence of the background, and photobleaching are not occurring. A microplate luminescence/fluorescence reader is one of the major components of the BRET imaging microscopy system, and the

acceptor fluorescence is detected as readout. BRET allows determination of the affinity of a small molecule for the target protein and the study of the intracellular residence time of inhibitors using kinetic measurements. This method was exploited to prove the isoenzyme-specific engagement of histone deacetylase inhibitors<sup>144</sup> and ligand engagement of G-protein-coupled receptors ( $\beta_2$ -adrenergic and adenosine receptors).<sup>145</sup> Roberts et al. exploited a NanoLuc small luciferase protein (19 kDa) as a BRET donor instead of luciferase (Luc), since it showed a higher fluorescence yield, a narrow spectrum, and a stable luminescence. As a BRET acceptor, the non-chloro-TOM dye (NCT), showing membrane permeability and significant spectral resolution, was employed. To explore the interaction of intracellular engagement of HDAC inhibitors, the hydroxamate-based inhibitor (SAHA) was conjugated with NCT and was used as displacement substrate (tracer displacement by unlabeled compounds).<sup>144</sup>

The same authors reported the quantitative aspects relevant to fully characterize the engagement. Inside living cells, a NanoLuc-tagged intracellular protein of interest achieves a dynamic equilibrium with a cell-permeable fluorescent dye (tracer). After binding of an unlabeled small molecule, complex disruption leads to a loss of BRET signal that is detected in a microplate format (Figure 14). NanoBRET tracers are often produced starting from a drug or a tool compound and allow a quantitative measurement of the apparent affinity and a real-time assessment of the residence time.<sup>162</sup>

The BRET method was also adopted for the identification of antimicrobial hits targeting the protein–protein interaction between the initiation factor  $\sigma$  and the  $\beta'$ -subunit of bacterial RNA polymerase.<sup>70</sup> The study combined an *in silico* screening with an *in vivo* bioluminescence resonance energy transfer in yeast cells, showing the large applicability of this technology. One hit was identified and optimized using medicinal chemistry approaches.<sup>163</sup>

The description of the quantitative, real-time measurements of intracellular target engagement using energy transfer is reported, and NanoBRET tracers with optimized cell permeability have been developed and fully characterized (Figure 15a). Two main classes have been identified that represent robust

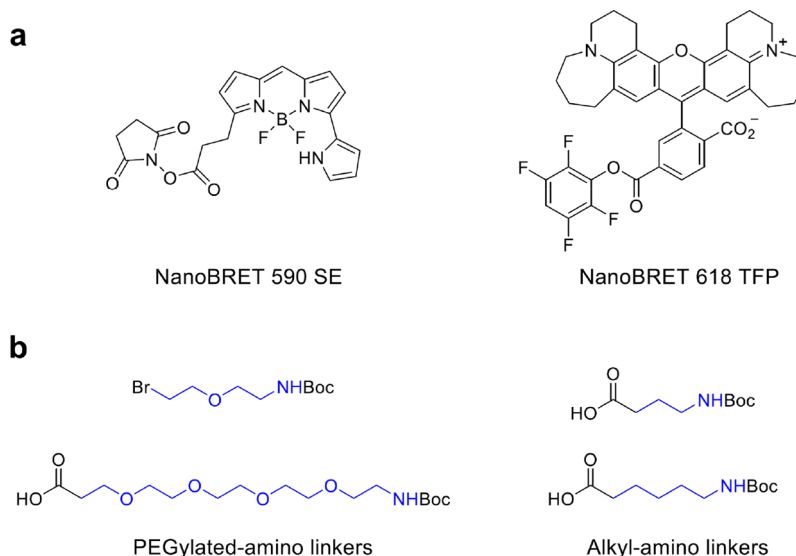


**Figure 15.** (a) Chemical structure of NanoBRET ester activated dyes; (b) example of linker building blocks. Dyes directly bound to the building block are known; however sometimes a linker (colored in blue) between the head tag and the fluorescent probe is necessary.

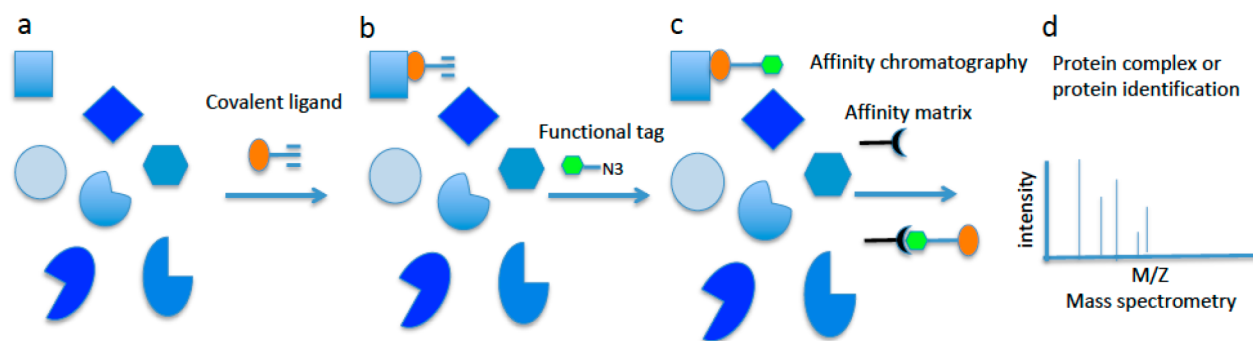


**Figure 16.** Example of ABCP process for covalently binding ligands. (a) Different targets available in the cells for binding the covalent ligand (orange) with the alkyne reactive functionality. (b) Covalent ligand binds the target and forms a covalent or noncovalent complex. The reactive group is exposed outside the binding site. (c) The functional tag (green) is added. It reacts with the reacting group of the covalent ligand (alkyne) with a click chemistry reaction, thus forming a covalent complex with the target. The green tag has a high affinity for the resin that should sequester the chimera–target complex from the sample matrix. (d) The affinity resin is added. The complex, once detached from the resin, is analyzed through mass spectrometry and the biomolecular target identified.

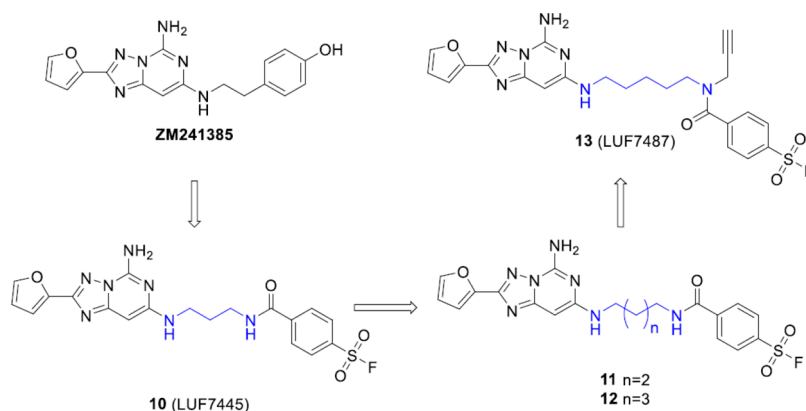


**Figure 17.** Chemical structures of the  $hA_{2A}R$  antagonists investigated by Yang et al. The selective  $hA_{2A}R$  antagonist (ZM241385) guided the design of the covalent antagonist **10**. The authors assessed the importance of the linker length (colored in blue) between the scaffold and the head on affinity and synthesized the optimized compounds **11** and **12**. Starting from compound **12**, the affinity-based probe **13** with an alkyne ligation-group and a fluorosulfonyl electrophilic was synthesized.

891 chemical tools for the assay. Linkers between the dye and the  
892 reacting group such as succinimide (NanoBRET 590 SE) or  
893 reactive esters (nanoBRET 618 TFP) can influence tracer  
894 properties, including affinity and cell permeability.

895 **4.4. A Chemical Proteomic Approach for Covalently**  
896 **Binding Ligands.** Affinity-based chemical proteomics (ABCP)  
897 is a method to study proteins or ligand–target interactions,  
898 based on protein isolation by an affinity reagent that can be  
899 coupled to a reporter system for detection. Affinity-based  
900 chemical proteomic has been used in target engagement studies  
901 of small-molecule drugs that covalently react with their targeted  
902 protein.<sup>164,165</sup> The compounds have a chimeric nature since a  
903 reactive functionality such as an alkyne (Figure 16a) or azide  
904 group is introduced in a suitable position of the scaffold. After  
905 addition to the cell, the ligand reacts with the protein target  
906 bearing a reactive group exposed and regioselectively placed.  
907 Both wild type and mutant proteins can be exploited for the  
908 study. When the functional tag (or affinity tag) is added to the  
909 cell, it binds to the covalent ligand through a click chemistry  
910 reaction (alkyne with azide, Figure 16b). “Click chemistry”<sup>20</sup> is  
911 exploited to attach *in situ* a functional tag, such as biotin. The  
912 functional tag allows affinity purification of the covalently bound  
913 protein of interest using, for example, streptavidin beads (Figure  
914 16c), and protein identification is performed using tryptic  
915 digestion and nanoliquid chromatography–tandem MS analysis

(Figure 16d). The functional tag presents a reactive head for the  
ligand and an affinity tag for the resin to allow affinity  
chromatography.

This method can be applied also to probes that bind proteins  
in a reversible fashion by the addition of a photoreactive group  
for UV detection of probe–protein interactions in cells (see  
photoaffinity labeling).<sup>166</sup> ABCP allows also off-targets  
detection in cells.<sup>167</sup>

Wong et al. investigated the specificity for a series of ATP-  
competitive bivalent kinase inhibitors targeting ABL1.<sup>168</sup> They  
proved the affinity and selectivity of bivalent inhibitors against  
Abl protein kinase with respect to other off-targets using dual  
functional chemical proteomics probes. A bivalent inhibitor A-2  
showed high affinity together with improved selectivity over the  
parental ATP-competitive inhibitor.

Another example of the pivotal role of chemical proteomic in  
chemical biology is the use of activity-based protein profiling  
(ABPP) to study proteins in their native environment.<sup>169</sup> By  
exploitation of click chemistry, an affinity-based probe for the  
human adenosine  $A_{2A}$  receptor ( $hA_{2A}R$ ) was developed to  
investigate the structural biology of the G-protein-coupled  
receptor (GPCR). Yang et al. developed compound **10**  
(LUF7445), a clickable affinity-based probe, with an electro-  
philic reactive group, as a covalent antagonist of  $hA_{2A}R$ .  
LUF7445 was discovered through chemical modification of 940

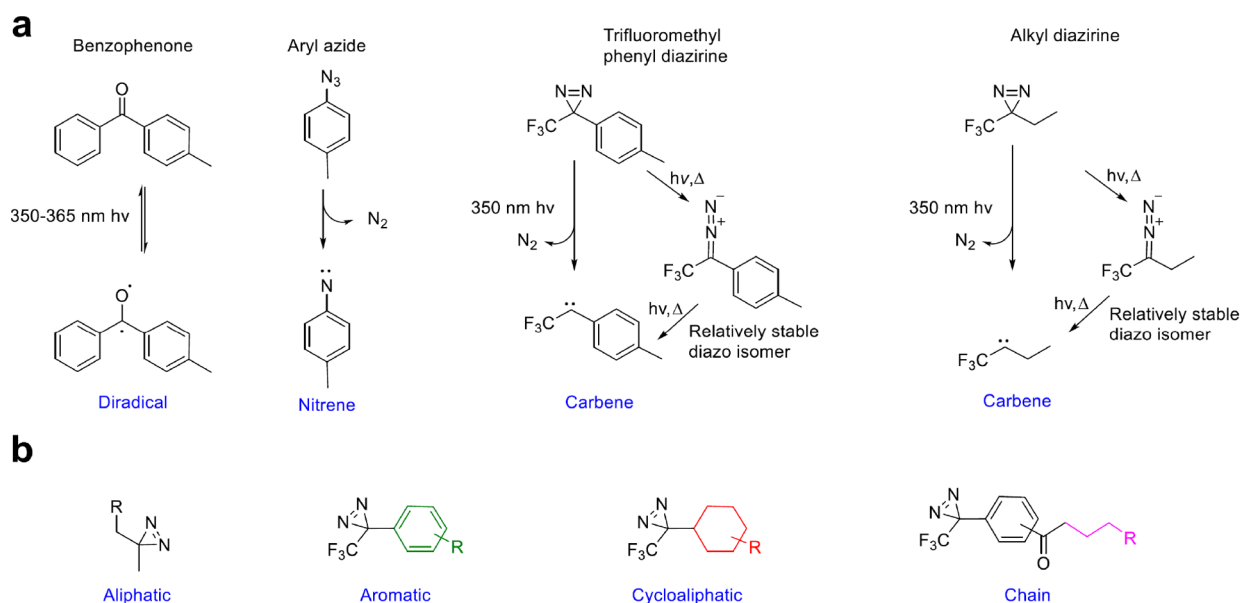


**Figure 18.** (a) Most relevant photoaffinity compounds used to tag protein ligands aiming to study target engagement, protein functions, and their photoreaction: benzophenone, aryl azide, and diazirine (trifluoromethylphenyl diazirine, trifluoromethylethyl diazirine). (b) General structures of scaffolds for photoaffinity tagging.

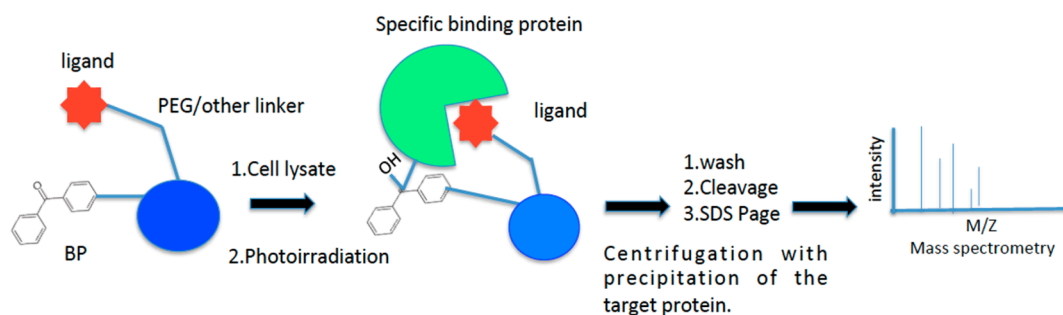


**Figure 19.** Efficient PAL method for protein identification using a bead-based multivalent probe.

941 compound ZM241385 introducing a fluorosulfonyl group, and  
 942 different linker lengths have been investigated. On the most  
 943 potent ligand, an alkyne-click handle was introduced leading to  
 944 the synthesis of probe **13** (Figure 17). The binding of the ligand  
 945 to the receptor was washout-resistant. This probe allowed  
 946 assessment of the presence of hA<sub>2A</sub>R in complex biological  
 947 samples. The identification of the affinity probe for a GPCR is a  
 948 promising tool to monitor the endogenous GPCR expression  
 949 related to human diseases.

950 **4.5. Photoaffinity Labeling.** Photoaffinity labeling (PAL)  
 951 is a well-known technique used to study specific protein function  
 952 or inhibition.<sup>170</sup> Photo-cross-linkers are conjugated with drugs  
 953 or substrates that can bind to the target protein (protein of  
 954 interest). Typically, photo-cross-linkers are (i) benzophenone  
 955 (BP), (ii) aryl azide (AA), and (iii) diazirine (DA) (Figure 18).  
 956 Upon photoirradiation, the photo-cross-linking functional  
 957 group generates highly reactive species that react with adjacent  
 958 molecules, leading to a direct covalent modification.<sup>171</sup>

959 PAL can capture partners through noncovalent interactions  
 960 and explore the ligand accessible protein space in a selective  
 961 mode. Photo-cross-linking agents have turned out to be essential  
 962 tools to study difficult targets such as protein–protein  
 963 interactions. Despite the high significance and extensive  
 964 application, only few photo-cross-linkers are currently available.  
 965 In the 1970s, BP has been introduced as a photo-cross-linker and

is the most used in PAL due to the good selectivity and affinity  
 toward methionine. Upon irradiation by 350–365 nm wave-  
 lengths, BP is converted into an active diradical. It reacts with  
 protein functional groups exploiting an abstraction–recombi-  
 nation reaction mechanism. Aryl azides cross-link through  
 nitrene, a reactive species, that is generated by loss of N<sub>2</sub> upon  
 photoirradiation with 254 and 400 nm wavelengths. Nitrene  
 reacts with nearby C–H and heteroatom–H bonds, creating a  
 novel covalent product. AAs are known to be chemically stable  
 and to have superior photophysical properties than the  
 corresponding acyl and alkyl analogs. Trifluoromethyl phenyl  
 DAs and alkyl DAs can both produce carbene as reactive species  
 losing N<sub>2</sub> upon photoirradiation at 350 nm. They can form  
 covalent adducts as phenyl diazirine (Figure 18a).<sup>172</sup> Novel  
 functionalized scaffold to be included in the chimeric  
 compounds can be designed starting from different precursor  
 reagents. In Figure 18b the colored fragments are included in the  
 final chemical photoaffinity reagent.

A typical methodology for target deconvolution in drug  
 discovery is applied to living cells or protein complexes,  
 including cell lysates, that are incubated with the compound.  
 The derivatized compound has a photoaffinity linker and a  
 reacting agent (drug, inhibitor, or ligand), and the compound–  
 protein binding is fixed by UV irradiation.<sup>173</sup> Affinity tag is used  
 to isolate proteins covalently bound to the compound, which are

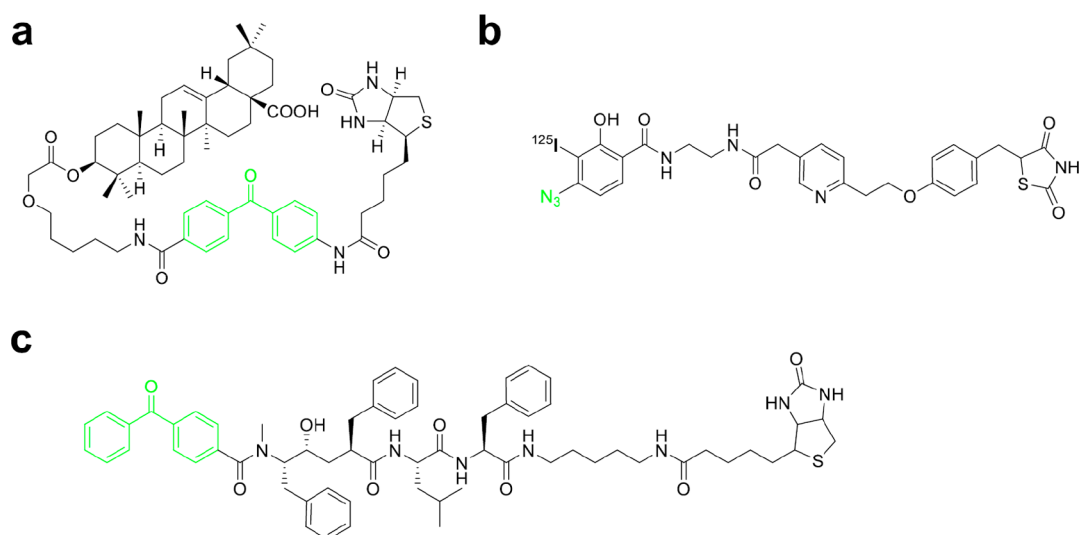


**Figure 20.** (a) Chimeric molecule designed to identify the target of oleanolic acid; (b) photoactivated- $\gamma$ -secretase inhibitor in which the tag covalently label presenilin 1; (c) photoaffinity labeled palmitoyl derivative directed to the peroxisomal  $\beta$ -oxidation enzyme. Shown in green are the photoreactive groups.

991 then analyzed exploiting MS-based proteomics for proteins  
992 identification (Figure 19). T. Tomohiro identified pyruvate  
993 carboxylase and C-terminal biotin carboxyl carrier protein as  
994 biotin-binding protein from HeLa cells using a PAL-based  
995 enrichment with an isotope-coded fluorescent and photo-  
996 cleavable tag followed by MS.<sup>174</sup> Relatively small functional  
997 groups for click chemistry have been recently introduced aimed  
998 at improving the photo-cross-linking yield and at gaining  
999 sensitivity of MS-based proteomics. This method could be  
1000 applied also when the affinity between the target protein and the  
1001 small molecule is weak.

1002 The Kaori Sakurai group used PAL to detect the binding  
1003 protein of benzenesulfonamide.<sup>175</sup> They produced trifunctional  
1004 probes bearing a lysine scaffold and containing a benzenesulfo-  
1005 namide moiety as protein-binding ligand. The photoactivatable  
1006 group was BP, and biotin was selected as reporter group,  
1007 allowing the detection of the protein-covalent adducts (Figure  
1008 19).

1009 Other engineered chimeric structures have been adopted for  
1010 tagging experiments. For example, a chimeric molecule to  
1011 identify the target of oleanolic acid was prepared<sup>176</sup> (Figure  
1012 20a), and a photoactivated  $\gamma$ -secretase inhibitor in which the tag  
1013 covalently label presenilin 1 was developed<sup>177</sup> (Figure 20b).  
1014 Presenilin 1 belongs to the  $\gamma$  secretase complex and plays an  
1015 important role in the generation of amyloid  $\beta$  ( $A\beta$ ) from the  
1016 amyloid precursor protein, and it is associated with the onset of  
1017 Alzheimer disease. The novel photoaffinity labeled palmitoyl  
1018 derivative (Figure 20c) is directed to the peroxisomal  $\beta$ -  
1019 oxidation enzyme, a primary enzyme for fatty acid degrada-  
1020 tion.<sup>178</sup>

1021 Recently a high number of PAL applications have been  
1022 published, underlining the increasing importance of this method  
1023 in drug discovery.

1024 Other technologies are under development within the  
1025 engagement technology field such as the carbene footprinting  
1026 technology.<sup>179,180</sup> An example is given by the differential protein  
1027 footprinting approach that adopted an efficient photoactivated  
1028 probe and used it in mass spectrometry to map the binding cleft  
1029 of lysozyme, as well as between UPS5, a deubiquitinating  
1030 enzyme, and a diubiquitin substrate.<sup>179</sup>

## 5. CONCLUSION

The development of new technologies and chemical biology  
strategies has largely stimulated medicinal chemists' creativity to  
design molecules that could meet the challenges that a drug  
encounters from the delivery to the patient up to target binding.

This ambitious task was initially addressed using simple  
structures with chemophysical properties suitable for cell  
membrane penetration. However, chemistry exploration and  
modular approaches led to the design of engineered constructs  
called chimeric molecules. Chimeras have been exploited in a  
wide range of applications, such as drug targeting and release,  
drug tracking and monitoring when tagged with fluorescent  
probes, target engagement, and mechanism of action clarifica-  
tion. Recently, engineered systems in which both compounds/  
drugs and proteins are chemically modified to give more specific  
and less invasive assays have been developed. Crucial is the role  
of the linking fragment connecting the functional head with the  
tag. Starting from a disulfide and an ester, the first linkers were  
based on the early concept of prodrugs, in which a cleavable  
bond could easily release the bioactive compound. Application  
of this linker chemistry was promising; however, the use of these  
systems was hampered by the risk of low specificity. Improved  
engineered compounds were developed, and linkers were  
recognized as an essential tool for structure-activity relationship  
studies of chimeric compounds and for providing the requested  
reactivity to conjugate the head and the tag. From a linear  
structure, such as PEG and alkyl chains with reactive groups at  
the two edges, a "three-dimensional" decoration of the chain is  
taking place to address the biological requirements, as observed  
in some ADCs. Irrespective of application field, chimeric  
molecules and linkers are conceptually related and can be  
exploited also in fields different from those mentioned in the  
present Perspective, including biosensors, biomarkers, and  
molecular machine. Chimeras are being developed by teamwork  
of medicinal chemists and chemical biologists and represent  
formidable tools for targeted therapies and personalized  
medicine.

## 1067 ■ AUTHOR INFORMATION

## 1068 Corresponding Author

1069 Maria P. Costi – Department of Life Sciences, University of  
1070 Modena and Reggio Emilia, 41125 Modena, Italy; [orcid.org/0000-0002-0443-5402](https://orcid.org/0000-0002-0443-5402);  
1071 Phone: +390592058579;  
1072 Email: [mariapaola.costi@unimore.it](mailto:mariapaola.costi@unimore.it)

## 1073 Authors

1074 Chiara Borsari – Department of Biomedicine, University of Basel,  
1075 4058 Basel, Switzerland; [orcid.org/0000-0002-4688-8362](https://orcid.org/0000-0002-4688-8362)

1076 Darci J. Trader – Department of Medicinal Chemistry and  
1077 Molecular Pharmacology, Purdue University, West Lafayette,  
1078 Indiana 47907, United States; [orcid.org/0000-0002-0607-1243](https://orcid.org/0000-0002-0607-1243)

1079 Annalisa Tait – Department of Life Sciences, University of  
1080 Modena and Reggio Emilia, 41125 Modena, Italy

1082 Complete contact information is available at:

1083 <https://pubs.acs.org/10.1021/acs.jmedchem.9b01456>

## 1084 Author Contributions

1085 The manuscript was written through contributions of all  
1086 authors. All authors have given approval to the final version of  
1087 the manuscript.

## 1088 Notes

1089 The authors declare no competing financial interest.

## 1090 Biographies

1091 Chiara Borsari is a medicinal chemist, working as postdoctoral fellow at  
1092 the University of Basel in the group of Prof. M. Wymann. Her research  
1093 is focused on the design and synthesis of small-molecule anticancer  
1094 agents. Her main goal is the development of irreversible inhibitors as a  
1095 novel strategy in targeted cancer therapy. She got her Ph.D. at the  
1096 University of Modena and Reggio Emilia. During her Ph.D., she has  
1097 joined the NHRF in Athens and the State University of New York at  
1098 Albany. She is also keen on communicating science to the public: she  
1099 created a short movie “Life in Colour”, explaining the advancements in  
1100 cancer research, and she is part of the European Federation for  
1101 Medicinal Chemistry Communication Team.

1102 Darci J. Trader received a Ph.D. in Chemistry under the direction of  
1103 Prof. Erin E. Carlson at Indiana University in 2013. Her postdoctoral  
1104 studies were at The Scripps Research Institute in the laboratory of Prof.  
1105 Thomas Kodadek. She began her independent career at Purdue  
1106 University in 2016. Her lab, which is in the Department of Medicinal  
1107 Chemistry and Molecular Pharmacology, is focused on developing  
1108 methods and probes to monitor or perturb both ubiquitin-dependent  
1109 and -independent proteasome activity.

1110 Annalisa Tait is an Associate Professor at the Department of Life  
1111 Sciences of the University of Modena and Reggio Emilia. She has a  
1112 broad experience in medicinal chemistry, and she is currently teaching  
1113 Medicinal Chemistry/Drug Analysis in Pharmacy and Biotechnology  
1114 degree courses, as well as in the Hospital Pharmacy School of  
1115 Specialization. She was Director of the Doctorate School in Science and  
1116 Technologies for Health Products. Her research is mainly focused on  
1117 synthesis, structural characterization, and evaluation of heterocyclic  
1118 derivatives as antiviral, phosphodiesterase inhibitors and ligands of  $\alpha$ , 5-  
1119 HT1A, NOP, and  $\sigma$  receptors.

1120 Maria P. Costi obtained her Ph.D. in Medicinal Chemistry at the  
1121 University of Modena and Reggio Emilia and was a Visiting Scientist at  
1122 the University of California, San Francisco. She is Professor of  
1123 Medicinal Chemistry at the Department of Life Sciences, leading the  
1124 integrated laboratory of drug discovery and biotechnology. She  
1125 published approximately 150 papers in international journals, deposited

20 patents, and serves as an editorial board member of different  
journals. Her research focus is on targeting the folate metabolism in  
different organisms for the discovery of anticancer, anti-infective drugs  
by combining medicinal chemistry and chemical biology tools. A  
second field of her research is the discovery of novel drugs for neglected  
tropical diseases. She coordinated many European and national  
projects.

## 1133 ■ ACKNOWLEDGMENTS

1134 We thank G. Ponterini for advice and discussions. This work was  
1135 supported by the Foundation for Cancer Research in Italy by  
1136 Grant AIRC IG16977 (to M.P.C.).

## 1137 ■ ABBREVIATIONS USED

1138 RME, receptor mediated endocytosis; ADC, antibody–drug  
1139 conjugate; CPP, cell-penetrating peptide; THP, tumor homing  
1140 peptide; mAbs, monoclonal antibodies; SDS–PAGE, sodium  
1141 dodecyl sulfate–polyacrylamide gel electrophoresis; GST,  
1142 glutathione; PROTAC, proteolysis targeting chimera; CRBN,  
1143 cereblon; TBAF, tetra-*n*-butylammonium fluoride; TR-FRET,  
1144 time-resolved Förster resonance energy transfer; BRET, bio-  
1145 luminescence resonance energy transfer; FLIM, fluorescence  
1146 lifetime imaging microscopy; BET protein, bromodomain and  
1147 extraterminal domain protein family; CDK9, cyclin dependent  
1148 kinase 9.

## 1149 ■ REFERENCES

- 1150 (1) Kuan, S. L.; Bergamini, F. R. G.; Weil, T. Functional protein  
1151 nanostructures: a chemical toolbox. *Chem. Soc. Rev.* **2018**, *47*, 9069–  
1152 9105.
- 1153 (2) (a) Corson, T. W.; Aberle, N.; Crews, C. M. Design and  
1154 applications of bifunctional small molecules: why two heads are better  
1155 than one. *ACS Chem. Biol.* **2008**, *3*, 677–692. (b) Lautenslager, G. T.;  
1156 Simpson, L. L. Chimeric molecules constructed with endogenous  
1157 substances. *Adv. Mol. Cell Biol.* **1994**, *9*, 233–262.
- 1158 (3) (a) Maniaci, C.; Ciulli, A. Bifunctional chemical probes inducing  
1159 protein-protein interactions. *Curr. Opin. Chem. Biol.* **2019**, *52*, 145–  
1160 156. (b) Gilad, Y.; Tuchinsky, H.; Ben-David, G.; Minnes, R.; Gancz,  
1161 A.; Senderowitz, H.; Luboshits, G.; Firer, M. A.; Gellerman, G.  
1162 Discovery of potent molecular chimera (CM358) to treat human  
1163 metastatic melanoma. *Eur. J. Med. Chem.* **2017**, *138*, 602–615.
- 1164 (4) Tashima, T. Effective cancer therapy based on selective drug  
1165 delivery into cells across their membrane using receptor-mediated  
1166 endocytosis. *Bioorg. Med. Chem. Lett.* **2018**, *28*, 3015–3024.
- 1167 (5) Lazny, R. Hydrazone linker units. In *Linker Strategies in Solid-Phase*  
1168 *Organic Synthesis*; Scott, P. J. H., Ed.; John Wiley & Sons, Ltd.:  
1169 Chichester, U.K., 2009; pp 303–315, DOI: [10.1002/9780470749043.ch10](https://doi.org/10.1002/9780470749043.ch10).
- 1170 (6) Enders, D.; Wortmann, L.; Peters, R. Recovery of carbonyl  
1171 compounds from *N,N*-dialkylhydrazones. *Acc. Chem. Res.* **2000**, *33* (3),  
1172 157–169.
- 1173 (7) Corbett, P. T.; Leclair, J.; Vial, L.; West, K. R.; Wietor, J.-L.;  
1174 Sanders, J. K. M.; Otto, S. Dynamic combinatorial chemistry. *Chem.*  
1175 *Rev.* **2006**, *106* (9), 3652–3711.
- 1176 (8) Dyniewicz, J.; Lipiński, P. F. J.; Kosson, P.; Leśniak, A.;  
1177 Bochyńska-Czyż, M.; Muchowska, A.; Tourwé, D.; Ballet, S.; Misicka,  
1178 A.; Lipkowski, A. W. Hydrazone linker as a useful tool for preparing  
1179 chimeric peptide/nonpeptide bifunctional compounds. *ACS Med.*  
1180 *Chem. Lett.* **2017**, *8* (1), 73–77.
- 1181 (9) Yang, Y.; Fonović, M.; Verhelst, S. H. L. Cleavable linkers in  
1182 chemical proteomics applications. *Methods Mol. Biol.* **2017**, *1491*, 185–  
1183 203.
- 1184 (10) Park, K. D.; Liu, R.; Kohn, H. Useful tools for biomolecule  
1185 isolation, detection, and identification: acylhydrazone-based cleavable  
1186 linkers. *Chem. Biol.* **2009**, *16* (7), 763–772.
- 1187

- 1188 (11) Dirksen, A.; Yegneswaran, S.; Dawson, P. E. Bisaryl hydrazones  
1189 as exchangeable biocompatible linkers. *Angew. Chem., Int. Ed.* **2010**, *49*  
1190 (11), 2023–2027.
- 1191 (12) Góngora-Benítez, M.; Tulla-Puche, J.; Albericio, F. Multifaceted  
1192 roles of disulfide bonds. Peptides as therapeutics. *Chem. Rev.* **2014**, *114*  
1193 (2), 901–926.
- 1194 (13) Kourra, C. M. B. K.; Cramer, N. Converting disulfide bridges in  
1195 native peptides to stable methylene thioacetals. *Chem. Sci.* **2016**, *7* (12),  
1196 7007–7012.
- 1197 (14) Vinther, T. N.; Pettersson, I.; Huus, K.; Schlein, M.; Steensgaard,  
1198 D. B.; Sørensen, A.; Jensen, K. J.; Kjeldsen, T.; Hubalek, F. Additional  
1199 disulfide bonds in insulin: prediction, recombinant expression, receptor  
1200 binding affinity, and stability. *Protein Sci. Publ. Protein Soc.* **2015**, *24* (5),  
1201 779–788.
- 1202 (15) Chen, X.; Bai, Y.; Zaro, J. L.; Shen, W.-C. Design of an in vivo  
1203 cleavable disulfide linker in recombinant fusion proteins. *BioTechniques*  
1204 **2010**, *49* (1), 513–518.
- 1205 (16) Chen, S.; Morales-Sanfrutos, J.; Angelini, A.; Cutting, B.; Heinis,  
1206 C. Structurally diverse cyclisation linkers impose different backbone  
1207 conformations in bicyclic peptides. *ChemBioChem* **2012**, *13* (7), 1032–  
1208 1038.
- 1209 (17) Tegge, W.; Bautsch, W.; Frank, R. Synthesis of cyclic peptides  
1210 and peptide libraries on a new disulfide linker. *J. Pept. Sci.* **2007**, *13* (10),  
1211 693–699.
- 1212 (18) Arnér, E. S. J.; Holmgren, A. Physiological functions of  
1213 thioredoxin and thioredoxin reductase: thioredoxin and thioredoxin  
1214 reductase. *Eur. J. Biochem.* **2000**, *267* (20), 6102–6109.
- 1215 (19) Garnett, M. C. Targeted drug conjugates: principles and  
1216 progress. *Adv. Drug Delivery Rev.* **2001**, *53* (2), 171–216.
- 1217 (20) Hein, C. D.; Liu, X.-M.; Wang, D. Click chemistry, a powerful  
1218 tool for pharmaceutical sciences. *Pharm. Res.* **2008**, *25* (10), 2216–  
1219 2230.
- 1220 (21) Hems, E. S.; Wagstaff, B. A.; Saalbach, G.; Field, R. A. CuAAC  
1221 click chemistry for the enhanced detection of novel alkyne-based  
1222 natural product toxins. *Chem. Commun.* **2018**, *54* (86), 12234–12237.
- 1223 (22) Jeon, H.; Lim, C.; Lee, J. M.; Kim, S. Chemical assay-guided  
1224 natural product isolation via solid-supported chemodosimetric  
1225 fluorescent probe. *Chem. Sci.* **2015**, *6* (5), 2806–2811.
- 1226 (23) Gao, J.; Mfuh, A.; Amako, Y.; Woo, C. M. Small molecule  
1227 interactome mapping by photoaffinity labeling reveals binding site  
1228 hotspots for the NSAIDs. *J. Am. Chem. Soc.* **2018**, *140* (12), 4259–  
1229 4268.
- 1230 (24) Sohn, C. H.; Agnew, H. D.; Lee, J. E.; Sweredoski, M. J.; Graham,  
1231 R. L. J.; Smith, G. T.; Hess, S.; Czerwiec, G.; Loo, J. A.; Heath, J. R.;  
1232 Deshaies, R. J.; Beauchamp, J. L. Designer reagents for mass  
1233 spectrometry-based proteomics: clickable cross-linkers for elucidation  
1234 of protein structures and interactions. *Anal. Chem.* **2012**, *84* (6), 2662–  
1235 2669.
- 1236 (25) Schiapparelli, L. M.; McClatchy, D. B.; Liu, H.-H.; Sharma, P.;  
1237 Yates, J. R.; Cline, H. T. Direct detection of biotinylated proteins by  
1238 mass spectrometry. *J. Proteome Res.* **2014**, *13* (9), 3966–3978.
- 1239 (26) Wright, M. H.; Sieber, S. A. Chemical proteomics approaches for  
1240 identifying the cellular targets of natural products. *Nat. Prod. Rep.* **2016**,  
1241 *33* (5), 681–708.
- 1242 (27) Harju, K.; Vahermo, M.; Mutikainen, I.; Yli-Kauhaluoma, J.  
1243 Solid-phase synthesis of 1,2,3-triazoles via 1,3-dipolar cycloaddition. *J.*  
1244 *Comb. Chem.* **2003**, *5* (6), 826–833.
- 1245 (28) Blass, B. E.; Coburn, K. R.; Faulkner, A. L.; Hunn, C. L.; Natchus,  
1246 M. G.; Parker, M. S.; Portlock, D. E.; Tullis, J. S.; Wood, R. Solid-phase  
1247 synthesis of functionalized 1,2,3-triazoles. *Tetrahedron Lett.* **2002**, *43*  
1248 (22), 4059–4061.
- 1249 (29) Angelo, N. G.; Arora, P. S. Solution- and solid-phase synthesis of  
1250 triazole oligomers that display protein-like functionality. *J. Org. Chem.*  
1251 **2007**, *72* (21), 7963–7967.
- 1252 (30) Galibert, M.; Piller, V.; Piller, F.; Aucagne, V.; Delmas, A. F.  
1253 Combining triazole ligation and enzymatic glycosylation on solid phase  
1254 simplifies the synthesis of very long glycoprotein analogues. *Chem. Sci.*  
1255 **2015**, *6* (6), 3617–3623.
- (31) Rossin, R.; van Duijnhoven, S. M. J.; ten Hoeve, W.; Janssen, H. 1256  
M.; Kleijn, L. H. J.; Hoeben, F. J. M.; Versteegen, R. M.; Robillard, M. S. 1257  
Triggered drug release from an antibody–drug conjugate using fast 1258  
“click-to-release” chemistry in mice. *Bioconjugate Chem.* **2016**, *27* (7), 1259  
1697–1706. 1260
- (32) Versteegen, R. M.; Rossin, R.; tenHoeve, W.; Janssen, H. M.; 1261  
Robillard, M. S. Click to release: instantaneous doxorubicin elimination 1262  
upon tetrazine ligation. *Angew. Chem., Int. Ed.* **2013**, *52* (52), 14112– 1263  
14116. 1264
- (33) Sherman, E. J.; Lorenz, D. A.; Garner, A. L. Click chemistry- 1265  
mediated complementation assay for RNA–protein interactions. *ACS* 1266  
*Comb. Sci.* **2019**, *21* (7), 522–527. 1267
- (34) Lorenz, D. A.; Garner, A. L. A click chemistry-based microRNA 1268  
maturation assay optimized for high-throughput screening. *Chem.* 1269  
*Commun.* **2016**, *52* (53), 8267–8270. 1270
- (35) Zhang, C.; Han, X.-R.; Yang, X.; Jiang, B.; Liu, J.; Xiong, Y.; Jin, J. 1271  
Proteolysis targeting chimeras (PROTACs) of anaplastic lymphoma 1272  
kinase (ALK). *Eur. J. Med. Chem.* **2018**, *151*, 304–314. 1273
- (36) Wang, L.; Guillen, V. S.; Sharma, N.; Flessa, K.; Min, J.; Carlson, 1274  
K. E.; Toy, W.; Braji, S.; Katzenellenbogen, B. S.; Katzenellenbogen, J. 1275  
A.; Chandralapaty, S.; Sharma, A. A new class of selective estrogen 1276  
receptor degraders (SERDs): expanding the toolbox of PROTAC 1277  
degrons. *ACS Med. Chem. Lett.* **2018**, *9* (8), 803–808. 1278
- (37) Hines, J.; Lartigue, S.; Dong, H.; Qian, Y.; Crews, C. M. MDM2- 1279  
recruiting PROTAC offers superior, synergistic antiproliferative activity 1280  
via simultaneous degradation of BRD4 and stabilization of p53. *Cancer* 1281  
*Res.* **2019**, *79* (1), 251–262. 1282
- (38) Wurz, R. P.; Cee, V. J. Targeted degradation of MDM2 as a new 1283  
approach to improve the efficacy of MDM2-p53 inhibitors. *J. Med.* 1284  
*Chem.* **2019**, *62* (2), 445–447. 1285
- (39) Silva, M. C.; Ferguson, F. M.; Cai, Q.; Donovan, K. A.; Nandi, G.; 1286  
Patnaik, D.; Zhang, T.; Huang, H.-T.; Lucente, D. E.; Dickerson, B. C.; 1287  
Mitchison, T. J.; Fischer, E. S.; Gray, N. S.; Haggarty, S. J. Targeted 1288  
degradation of aberrant tau in frontotemporal dementia patient-derived 1289  
neuronal cell models. *eLife* **2019**, *8*, No. e45457. 1290
- (40) Cyrus, K.; Wehenkel, M.; Choi, E.-Y.; Han, H.-J.; Lee, H.; 1291  
Swanson, H.; Kim, K.-B. Impact of linker length on the activity of 1292  
PROTACs. *Mol. BioSyst.* **2011**, *7* (2), 359–364. 1293
- (41) Steinebach, C.; Lindner, S.; Udeshi, N. D.; Mani, D. C.; Kehm, 1294  
H.; Köpff, S.; Carr, S. A.; Gütschow, M.; Krönke, J. Homo-PROTACs 1295  
for the chemical knockdown of cereblon. *ACS Chem. Biol.* **2018**, *13* (9), 1296  
2771–2782. 1297
- (42) Lai, A. C.; Toure, M.; Hellerschmied, D.; Salami, J.; Jaime- 1298  
Figuerola, S.; Ko, E.; Hines, J.; Crews, C. M. Modular PROTAC design 1299  
for the degradation of oncogenic BCR-ABL. *Angew. Chem., Int. Ed.* 1300  
**2016**, *55* (2), 807–810. 1301
- (43) Zorba, A.; Nguyen, C.; Xu, Y.; Starr, J.; Borzilleri, K.; Smith, J.; 1302  
Zhu, H.; Farley, K. A.; Ding, W.; Schiemer, J.; Feng, X.; Chang, J. S.; 1303  
Uccello, D. P.; Young, J. A.; Garcia-Irrizary, C. N.; Czabaniuk, L.; 1304  
Schuff, B.; Oliver, R.; Montgomery, J.; Hayward, M. M.; Coe, J.; Chen, 1305  
J.; Niosi, M.; Luthra, S.; Shah, J. C.; El-Kattan, A.; Qiu, X.; West, G. M.; 1306  
Noe, M. C.; Shanmugasundaram, V.; Gilbert, A. M.; Brown, M. F.; 1307  
Calabrese, M. F. Delineating the role of cooperativity in the design of 1308  
potent PROTACs for BTK. *Proc. Natl. Acad. Sci. U. S. A.* **2018**, *115* 1309  
(31), E7285–E7292. 1310
- (44) Ma, B.; Tsai, C.-J.; Haliloğlu, T.; Nussinov, R. Dynamic allostery: 1311  
linkers are not merely flexible. *Structure* **2011**, *19* (7), 907–917. 1312
- (45) Odendaal, A. Y.; Trader, D. J.; Carlson, E. E. Chemoselective 1313  
enrichment for natural products discovery. *Chem. Sci.* **2011**, *2* (4), 1314  
760–764. 1315
- (46) Trader, D. J.; Carlson, E. E. Siloxyl ether functionalized resins for 1316  
chemoselective enrichment of carboxylic acids. *Org. Lett.* **2011**, *13* (20), 1317  
5652–5655. 1318
- (47) Trader, D. J.; Carlson, E. E. Taming of a superbase for selective 1319  
phenol desilylation and natural product isolation. *J. Org. Chem.* **2013**, *78* 1320  
(14), 7349–7355. 1321
- (48) Trader, D. J.; Carlson, E. E. Toward the development of solid- 1322  
supported reagents for separation of alcohol-containing compounds by 1323  
steric environment. *Tetrahedron* **2014**, *70* (27–28), 4191–4196. 1324

- (49) Capehart, S. L.; Carlson, E. E. Mass spectrometry-based assay for the rapid detection of thiol-containing natural products. *Chem. Commun.* **2016**, *52* (90), 13229–13232.
- (50) Cox, C. L.; Tietz, J. I.; Sokolowski, K.; Melby, J. O.; Doroghazi, J. R.; Mitchell, D. A. Nucleophilic 1,4-additions for natural product discovery. *ACS Chem. Biol.* **2014**, *9* (9), 2014–2022.
- (51) Castro-Falcón, G.; Hahn, D.; Reimer, D.; Hughes, C. C. Thiol probes to detect electrophilic natural products based on their mechanism of action. *ACS Chem. Biol.* **2016**, *11* (8), 2328–2336.
- (52) Rudolf, G. C.; Koch, M. F.; Mandl, F. A. M.; Sieber, S. A. Subclass-specific labeling of protein-reactive natural products with customized nucleophilic probes. *Chem. - Eur. J.* **2015**, *21* (9), 3701–3707.
- (53) Rohena, C. C.; Mooberry, S. L. Recent progress with microtubule stabilizers: new compounds, binding modes and cellular activities. *Nat. Prod. Rep.* **2014**, *31* (3), 335–355.
- (54) Komlodi-Pasztor, E.; Sackett, D.; Wilkerson, J.; Fojo, T. Mitosis is not a key target of microtubule agents in patient tumors. *Nat. Rev. Clin. Oncol.* **2011**, *8* (4), 244–250.
- (55) Lee, M. M.; Gao, Z.; Peterson, B. R. Synthesis of a fluorescent analogue of paclitaxel that selectively binds microtubules and sensitively detects efflux by P-glycoprotein. *Angew. Chem., Int. Ed.* **2017**, *56* (24), 6927–6931.
- (56) Obeng, E. A.; Carlson, L. M.; Gutman, D. M.; Harrington, W. J.; Lee, K. P.; Boise, L. H. Proteasome inhibitors induce a terminal unfolded protein response in multiple myeloma cells. *Blood* **2006**, *107* (12), 4907–4916.
- (57) Orłowski, R. Z.; Kuhn, D. J. Proteasome inhibitors in cancer therapy: lessons from the first decade. *Clin. Cancer Res.* **2008**, *14* (6), 1649–1657.
- (58) Oerlemans, R.; Franke, N. E.; Assaraf, Y. G.; Cloos, J.; van Zantwijk, I.; Berkers, C. R.; Scheffer, G. L.; Debipersad, K.; Vojtekova, K.; Lemos, C.; van der Heijden, J. W.; Ylstra, B.; Peters, G. J.; Kaspers, G. L.; Dijkmans, B. A.; Scheper, R. J.; Jansen, G. Molecular basis of bortezomib resistance: proteasome subunit 5 (PSMB5) gene mutation and overexpression of PSMB5 protein. *Blood* **2008**, *112* (6), 2489–2499.
- (59) Carmony, K. C.; Kim, K. B. Activity-based imaging probes of the proteasome. *Cell Biochem. Biophys.* **2013**, *67* (1), 91–101.
- (60) de Jong, A.; Schuurman, K. G.; Rodenko, B.; Ovaa, H.; Berkers, C. R. Fluorescence-based proteasome activity profiling. *Methods Mol. Biol.* **2012**, *803*, 183–204.
- (61) Florea, B. I.; Verdoes, M.; Li, N.; van der Linden, W. A.; Geurink, P. P.; van den Elst, H.; Hofmann, T.; de Ru, A.; van Veelen, P. A.; Tanaka, K.; Sasaki, K.; Murata, S.; den Dulk, H.; Brouwer, J.; Ossendorp, F. A.; Kisselev, A. F.; Overkleeft, H. S. Activity-based profiling reveals reactivity of the murine thymoproteasome-specific 1371 subunit  $\beta 5t$ . *Chem. Biol.* **2010**, *17* (8), 795–801.
- (62) Ovaa, H.; van Swieten, P. F.; Kessler, B. M.; Leeuwenburgh, M. A.; Fiebiger, E.; van den Nieuwendijk, A. M. C. H.; Galaray, P. J.; van der Marel, G. A.; Ploegh, H. L.; Overkleeft, H. S. Chemistry in living cells: detection of active proteasomes by a two-step labeling strategy. *Angew. Chem., Int. Ed.* **2003**, *42* (31), 3626–3629.
- (63) Verdoes, M.; Hillaert, U.; Florea, B. I.; Sae-Heng, M.; Risseuw, M. D. P.; Filipov, D. V.; van der Marel, G. A.; Overkleeft, H. S. Acetylene functionalized BODIPY dyes and their application in the synthesis of activity based proteasome probes. *Bioorg. Med. Chem. Lett.* **2007**, *17* (22), 6169–6171.
- (64) de Bruin, G.; Xin, B. T.; Kraus, M.; van der Stelt, M.; van der Marel, G. A.; Kisselev, A. F.; Driessen, C.; Florea, B. I.; Overkleeft, H. S. A set of activity-based probes to visualize human (immuno)proteasome activities. *Angew. Chem., Int. Ed.* **2016**, *55* (13), 4199–4203.
- (65) Jen, E. Y.; Ko, C. W.; Lee, J. E.; Del Valle, P. L.; Aydanian, A.; Jewell, C.; Norsworthy, K. J.; Przepiorka, D.; Nie, L.; Liu, J.; Sheth, C. M.; Shapiro, M.; Farrell, A. T.; Pazdur, R. FDA approval: gemtuzumab ozogamicin for the treatment of adults with newly diagnosed CD33-positive acute myeloid leukemia. *Clin. Cancer Res.* **2018**, *24*, 3242–3246.
- (66) Norsworthy, K. J.; Ko, C. W.; Lee, J. E.; Liu, J.; John, C. S.; Przepiorka, D.; Farrell, A. T.; Pazdur, R. FDA approval summary: mylotarg for treatment of patients with relapsed or refractory CD33-positive acute myeloid leukemia. *Oncologist* **2018**, *23*, 1103–1108.
- (67) Lamb, Y. N. Inotuzumab ozogamicin: first global approval. *Drugs* **2017**, *77*, 1603–1610.
- (68) Donato, E. M.; Fernández-Zaroso, M.; Hueso, J. A.; de la Rubia, J. Brentuximab vedotin in Hodgkin lymphoma and anaplastic large-cell lymphoma: an evidence-based review. *OncoTargets Ther.* **2018**, *11*, 4583–4590.
- (69) Richardson, N. C.; Kasamon, Y. L.; Chen, H.; de Claro, R. A.; Ye, J.; Blumenthal, G. M.; Farrell, A. T.; Pazdur, R. FDA approval summary: brentuximab vedotin in first-line treatment of peripheral T-cell lymphoma. *Oncologist* **2019**, *24*, e180–e187.
- (70) von Minckwitz, G.; Huang, C. S.; Mano, M. S.; Loibl, S.; Mamounas, E. P.; Untch, M.; Wolmark, N.; Rastogi, P.; Schneeweiss, A.; Redondo, A.; Fischer, H. H.; Jacot, W.; Conlin, A. K.; Arce-Salinas, C.; Wapnir, I. L.; Jackisch, C.; DiGiovanna, M. P.; Fasching, P. A.; Crown, J. P.; Wülfing, P.; Shao, Z.; Rota Caremoli, E.; Wu, H.; Lam, L. H.; Tesarowski, D.; Smitt, M.; Douthwaite, H.; Singel, S. M.; Geyer, C. E., Jr. KATHERINE Investigators. Trastuzumab emtansine for residual invasive HER2-positive breast cancer. *N. Engl. J. Med.* **2019**, *380*, 617–628.
- (71) Verma, S.; Miles, D.; Gianni, L.; Krop, I. E.; Welslau, M.; Baselga, J.; Pegram, M.; Oh, D. Y.; Diéras, V.; Guardino, E.; Fang, L.; Lu, M. W.; Olsen, S.; Blackwell, K. EMILIA Study Group. Trastuzumab emtansine for HER2-positive advanced breast cancer. *N. Engl. J. Med.* **2012**, *367*, 1783–1791.
- (72) Deeks, E. D. Polatuzumab vedotin: first global approval. *Drugs* **2019**, *79* (13), 1467–1475.
- (73) Sacchi, A.; Gasparri, A.; Curnis, F.; Bellone, M.; Corti, A. Crucial role for interferon gamma in the synergism between tumor vasculature-targeted tumor necrosis factor alpha (NGR-TNF) and doxorubicin. *Cancer Res.* **2004**, *64*, 7150–7155.
- (74) Gregorc, V.; Cavina, R.; Novello, S.; Grossi, F.; Lazzari, C.; Capelletto, E.; Genova, C.; Salini, G.; Lambiase, A.; Santoro, A. NGR-hTNF and doxorubicin as second-line treatment of patients with small cell lung cancer. *Oncologist* **2018**, *23*, 1133–e112.
- (75) Chen, H.; Niu, G.; Wu, H.; Chen, X. Clinical application of radiolabeled RGD peptides for PET imaging of integrin  $\alpha v\beta 3$ . *Theranostics* **2016**, *6*, 78–92.
- (76) Sehnert, B.; Burkhardt, H.; Dübel, S.; Voll, R. E. The “sneaking-ligand” approach: cell-type specific inhibition of the classical NF- $\kappa$ B pathway. *Methods Mol. Biol.* **2015**, *1280*, 559–578.
- (77) Kawaguchi, Y.; Takeuchi, T.; Kuwata, K.; Chiba, J.; Hatanaka, Y.; Nakase, I.; Futaki, S. Syndecan-4 is a receptor for clathrin-mediated endocytosis of arginine-rich cell-penetrating peptides. *Bioconjugate Chem.* **2016**, *27*, 1119–1130.
- (78) Milletti, F. Cell-penetrating peptides: classes, origin, and current landscape. *Drug Discovery Today* **2012**, *17*, 850–860.
- (79) Pooga, M.; Langel, U. Classes of cell-penetrating peptides. *Methods Mol. Biol.* **2015**, *1324*, 3–28.
- (80) Lönn, P.; Dowdy, S. F. Cationic PTD/PPP-mediated macromolecular delivery: charging into the cell. *Expert Opin. Drug Delivery* **2015**, *12*, 1627–1636.
- (81) Becker-Hapak, M.; McAllister, S. S.; Dowdy, S. F. TAT-mediated protein transduction into mammalian cells. *Methods* **2001**, *24*, 247–256.
- (82) Klein, M. J.; Schmidt, S.; Wadhvani, P.; Bürck, J.; Reichert, J.; Afonin, S.; Berditsch, M.; Schober, T.; Brock, R.; Kansy, M.; Ulrich, A. S. Lactam-stapled cell-penetrating peptides: cell uptake and membrane binding properties. *J. Med. Chem.* **2017**, *60*, 8071–8082.
- (83) Mitchell, D. J.; Kim, D. T.; Steinman, L.; Fathman, C. G.; Rothbard, J. B. Polyarginine enters cells more efficiently than other polycationic homopolymers. *J. Pept. Res.* **2000**, *56*, 318–325.
- (84) Kalafatovic, D.; Giral, E. Cell-penetrating peptides: design strategies beyond primary structure and amphipathicity. *Molecules* **2017**, *22* (11), 1929.

- (85) Yang, T.; Li, F.; Zhang, H.; Fan, L.; Qiao, Y.; Tan, G.; Zhang, H.; Wu, H. Multifunctional pH-sensitive micelles for tumor-specific uptake and cellular delivery. *Polym. Chem.* **2015**, *6*, 1373–1382.
- (86) Bhunia, D.; Mondal, P.; Das, G.; Saha, A.; Sengupta, P.; Jana, J.; Mohapatra, S.; Chatterjee, S.; Ghosh, S. Spatial position regulates power of tryptophan: discovery of a major-groove-specific nuclear-localizing, cell-penetrating tetrapeptide. *J. Am. Chem. Soc.* **2018**, *140*, 1697–1714.
- (87) Dominguez-Berrocal, L.; Cirri, E.; Zhang, X.; Andriani, L.; Marin, G. H.; Lebel-Binay, S.; Rebollo, A. New therapeutic approach for targeting Hippo signaling pathway. *Sci. Rep.* **2019**, *9* (1), 4771.
- (88) (a) Veiman, K. L.; Mager, I.; Ezzat, K.; Margus, H.; Lehto, T.; Langel, K.; Kurrikoff, K.; Arukuusk, P.; Suhorutsenko, J.; Padari, K.; Pooga, M.; Lehto, T.; Langel, Ü. PepFect14 peptide vector for efficient gene delivery in cell cultures. *Mol. Pharmaceutics* **2013**, *10*, 199–210. (b) Ezzat, K.; El Andaloussi, S.; Zaghloul, E. M.; Lehto, T.; Lindberg, S.; Moreno, P. M.; Viola, J. R.; Magdy, T.; Abdo, R.; Guterstam, P.; Sillard, R.; Hammond, S. M.; Wood, M. J.; Arzumanov, A. A.; Gait, M. J.; Smith, C. I.; Hällbrink, M.; Langel, Ü. PepFect 14, a novel cell-penetrating peptide for oligonucleotide delivery in solution and as solid formulation. *Nucleic Acids Res.* **2011**, *39* (12), 5284–5298.
- (89) (a) Ezzat, K.; Helmfors, H.; Tudoran, O.; Juks, C.; Lindberg, S.; Padari, K.; El-Andaloussi, S.; Pooga, M.; Langel, U. Scavenger receptor-mediated uptake of cell-penetrating peptide nanocomplexes with oligonucleotides. *FASEB J.* **2012**, *26*, 1172–1180. (b) Lindberg, S.; Muñoz-Alarcón, A.; Helmfors, H.; Mosqueira, D.; Gyllborg, D.; Tudoran, O.; Langel, U. PepFect15, a novel endosomolytic cell-penetrating peptide for oligonucleotide delivery via scavenger receptors. *Int. J. Pharm.* **2013**, *441*, 242–247.
- (90) Lindberg, S.; Regberg, J.; Eriksson, J.; Helmfors, H.; Munoz-Alarcon, A.; Srimanee, A.; Figueroa, R. A.; Hallberg, E.; Ezzat, K.; Langel, U. A convergent uptake route for peptide- and polymer-based nucleotide delivery systems. *J. Controlled Release* **2015**, *206*, 58–66.
- (91) Craig, A. J.; Meloni, B. P.; Watt, P. M.; Knuckey, N. W. Attenuation of neuronal death by peptide inhibitors of AP-1 activation in acute and delayed in vitro ischaemia (oxygen/glucose deprivation) models. *Int. J. Pept. Res. Ther.* **2011**, *17*, 1–6.
- (92) Vaslin, A.; Puyal, J.; Clarke, P. G. Excitotoxicity-induced endocytosis confers drug targeting in cerebral ischemia. *Ann. Neurol.* **2009**, *65*, 337–347.
- (93) Meloni, B. P.; Brookes, L. M.; Clark, V. W.; Cross, J. L.; Edwards, A. B.; Anderton, R. S.; Hopkins, R. M.; Hoffmann, K.; Knuckey, N. W. Poly-arginine and arginine-rich peptides are neuroprotective in stroke models. *J. Cereb. Blood Flow Metab.* **2015**, *35*, 993–1004.
- (94) Lang, B. T.; Cregg, J. M.; DePaul, M. A.; Tran, A. P.; Xu, K.; Dyck, S. M.; Madalena, K. M.; Brown, B. P.; Weng, Y. L.; Li, S.; Karimi-Abdolrezaee, S.; Busch, S. A.; Shen, Y.; Silver, J. Modulation of the proteoglycan receptor PTP $\sigma$  promotes recovery after spinal cord injury. *Nature* **2015**, *518*, 404–408.
- (95) Wadia, J. S.; Stan, R. V.; Dowdy, S. F. Transducible TAT-HA fusogenic peptide enhances escape of TAT-fusion proteins after lipid raft macropinocytosis. *Nat. Med.* **2004**, *10*, 310–315.
- (96) Richard, J. P.; Melikov, K.; Brooks, H.; Prevot, P.; Lebleu, B.; Chernomordik, L. V. Cellular uptake of unconjugated TAT peptide involves clathrin-dependent endocytosis and heparan sulfate receptors. *J. Biol. Chem.* **2005**, *280*, 15300–15306.
- (97) Ferrari, A.; Pellegrini, V.; Arcangeli, C.; Fittipaldi, A.; Giacca, M.; Beltram, F. Caveolae-mediated internalization of extracellular HIV-1 tat fusion proteins visualized in real time. *Mol. Ther.* **2003**, *8*, 284–294.
- (98) Kosuge, M.; Takeuchi, T.; Nakase, I.; Jones, A. T.; Futaki, S. Cellular internalization and distribution of arginine-rich peptides as a function of extracellular peptide concentration, serum, and plasma membrane associated proteoglycans. *Bioconjugate Chem.* **2008**, *19*, 656–664.
- (99) Labropoulou, V. T.; Skandalis, S. S.; Ravazoula, P.; Perimenis, P.; Karamanos, N. K.; Kalofonos, H. P.; Theocharis, A. D. Expression of syndecan-4 and correlation with metastatic potential in testicular germ cell tumours. *BioMed Res. Int.* **2013**, *2013*, 214864.
- (100) Baba, F.; Swartz, K.; van Buren, R.; Eickhoff, J.; Zhang, Y.; Wolberg, W.; Friedl, A. Syndecan-1 and syndecan-4 are overexpressed in an estrogen receptor-negative, highly proliferative breast carcinoma subtype. *Breast Cancer Res. Treat.* **2006**, *98*, 91–98.
- (101) Yung, S.; Woods, A.; Chan, T. M.; Davies, M.; Williams, J. D.; Couchman, J. R. Syndecan-4 up-regulation in proliferative renal disease is related to microfilament organization. *FASEB J.* **2001**, *15*, 1631–1633.
- (102) Rodriguez Plaza, J. G.; Morales-Nava, R.; Diener, C.; Schreiber, G.; Gonzalez, Z. D.; Ortiz, M. T. L.; Blake, I. O.; Pantoja, O.; Volkmer, R.; Klipp, E.; Herrmann, A.; Del Rio, G. Cell penetrating peptides and cationic antibacterial peptides: two sides of the same coin. *J. Biol. Chem.* **2014**, *289*, 14448–14457.
- (103) Li, L.; Shi, Y.; Su, G.; Le, G. Selectivity for and destruction of Salmonella typhimurium via a membrane damage mechanism of a cell penetrating peptide ppTG20 analogue. *Int. J. Antimicrob. Agents* **2012**, *40*, 337–343.
- (104) Gautam, A.; Kapoor, P.; Chaudhary, K.; Kumar, R.; Open Source Drug Discovery Consortium; Raghava, G. P. S. Tumor homing peptides as molecular probes for cancer therapeutics, diagnostics and theranostics. *Curr. Med. Chem.* **2014**, *21*, 2367–2391.
- (105) Fan, L. Q.; Du, G. X.; Li, P. F.; Li, M. W.; Sun, Y.; Zhao, L. M. Improved breast cancer cell-specific intracellular drug delivery and therapeutic efficacy by coupling decoration with cell penetrating peptide and SP90 peptide. *Biomed. Pharmacother.* **2016**, *84*, 1783–1791.
- (106) Lu, L.; Qi, H.; Zhu, J.; Sun, W. X.; Zhang, B.; Tang, C. Y.; Cheng, Q. Vascular-homing peptides for cancer therapy. *Biomed. Pharmacother.* **2017**, *92*, 187–195.
- (107) Gregorc, V.; Santoro, A.; Bennicelli, E.; Punt, C. J.; Citterio, G.; Timmer-Bonte, J. N.; Caligaris Cappio, F.; Lambiase, A.; Bordignon, C.; van Herpen, C. M. Phase Ib study of NGR-hTNF, a selective vascular targeting agent, administered at low doses in combination with doxorubicin to patients with advanced solid tumours. *Br. J. Cancer* **2009**, *101*, 219–224.
- (108) Lorusso, D.; Scambia, G.; Amadio, G.; di Legge, A.; Pietragalla, A.; De Vincenzo, R.; Masciullo, V.; Di Stefano, M.; Mangili, G.; Citterio, G.; Mantori, M.; Lambiase, A.; Bordignon, C. Phase II study of NGR-hTNF in combination with doxorubicin in relapsed ovarian cancer patients. *Br. J. Cancer* **2012**, *107*, 37–42.
- (109) Gregorc, V.; Gaafar, R. M.; Favaretto, A.; Grossi, F.; Jassem, J.; Polychronis, A.; Bidoli, P.; Tiseo, M.; Shah, R.; Taylor, P.; Novello, S.; Muzio, A.; Bearz, A.; Greillier, L.; Fontana, F.; Salini, G.; Lambiase, A.; O'Brien, M. NGR-hTNF in combination with best investigator choice in previously treated malignant pleural mesothelioma (NGR015): a randomised, double-blind, placebo-controlled phase 3 trial. *Lancet Oncol.* **2018**, *19*, 799–811.
- (110) Zarovni, N.; Monaco, L.; Corti, A. Inhibition of tumor growth by intramuscular injection of cDNA encoding tumor necrosis factor alpha coupled to NGR and RGD tumor-homing peptides. *Hum. Gene Ther.* **2004**, *15*, 373–382.
- (111) Seidi, K.; Jahanban-Esfahlan, R.; Monhemi, H.; Zare, P.; Minofar, B.; Daei Farshchi Adli, A.; Farajzadeh, D.; Behzadi, R.; Mesgari Abbasi, M.; Neubauer, H. A.; Moriggl, R.; Zarghami, N.; Javaheri, T. NGR (Asn-Gly-Arg)-targeted delivery of coagulase to tumor vasculature arrests cancer cell growth. *Oncogene* **2018**, *37*, 3967–3980.
- (112) Hosseini, E.; Hosseini, S. Y.; Hashempour, T.; Fattahi, M. R.; Sadeghizadeh, M. Effect of RGD coupled MDA-7/IL-24 on apoptosis induction in a hepatocellular carcinoma cell line. *Mol. Med. Rep.* **2017**, *15*, 495–501.
- (113) Zhang, B. F.; Liu, J. J.; Pei, D. S.; Yang, Z. X.; Di, J. H.; Chen, F.; Li, H. Z.; Xu, W.; Wu, Y. P.; Zheng, J. N. Potent antitumor effect elicited by RGD-mda-7, an mda-7/IL-24 mutant, via targeting the integrin receptor of tumor cells. *Cancer Biother. Radiopharm.* **2011**, *26*, 647–655.
- (114) Bina, S.; Hosseini, S. Y.; Shenavar, F.; Hosseini, E.; Mortazavi, M. The effect of RGD/NGR peptide modification of melanoma differentiation-associated gene-7/interleukin-24 on its receptor attach-

- 1598 ment, an in silico analysis. *Cancer Biother.Radiopharm.* **2017**, *32*, 205–  
1599 214.
- 1600 (115) Numata, K.; Reagan, M. R.; Goldstein, R. H.; Rosenblatt, M.;  
1601 Kaplan, D. L. Spider silk-based gene carriers for tumor cell-specific  
1602 delivery. *Bioconjugate Chem.* **2011**, *22*, 1605–1610.
- 1603 (116) Bini, E.; Foo, C. W.; Huang, J.; Karageorgiou, V.; Kitchel, B.;  
1604 Kaplan, D. L. RGD-functionalized bioengineered spider dragline silk  
1605 biomaterial. *Biomacromolecules* **2006**, *7*, 3139–3145.
- 1606 (117) Huang, J.; Valluzzi, R.; Bini, E.; Vernaglia, B.; Kaplan, D. L.  
1607 Cloning, expression, and assembly of sericin-like protein. *J. Biol. Chem.*  
1608 **2003**, *278*, 46117–46123.
- 1609 (118) Prince, J. T.; McGrath, K. P.; DiGirolamo, C. M.; Kaplan, D. L.  
1610 Construction, cloning, and expression of synthetic genes encoding  
1611 spider dragline silk. *Biochemistry* **1995**, *34*, 10879–10885.
- 1612 (119) Yan, S. Z.; Beeler, J. A.; Chen, Y. B.; Shelton, R. K.; Tang, W. J.  
1613 The regulation of type 7 adenyllyl cyclase by its C1b region and  
1614 *Escherichia coli* peptidylprolyl isomerase, SlyD. *J. Biol. Chem.* **2001**, *276*,  
1615 8500–8506.
- 1616 (120) Galbiati, E.; Gambini, L.; Civitarese, V.; Bellini, M.; Ambrosini,  
1617 D.; Allevi, R.; Avvakumova, S.; Romeo, S.; Prosperi, D. “Blind” targeting  
1618 in action: from phage display to breast cancer cell targeting with  
1619 peptide-gold nanoconjugates. *Pharmacol. Res.* **2016**, *111*, 155–162.
- 1620 (121) Peters, C.; Brown, S. Antibody-drug conjugates as novel anti-  
1621 cancer chemotherapeutics. *Biosci. Rep.* **2015**, *35*, No. e00225.
- 1622 (122) Imamura, C. K. Therapeutic drug monitoring of monoclonal  
1623 antibodies: applicability based on their pharmacokinetic properties.  
1624 *Drug Metab. Pharmacokinet.* **2019**, *34*, 14–18.
- 1625 (123) Saeed, A. F.; Wang, R.; Ling, S.; Wang, S. Antibody engineering  
1626 for pursuing a healthier future. *Front. Microbiol.* **2017**, *8*, 495.
- 1627 (124) Reichert, J. M.; Dhimolea, E. The future of antibodies as cancer  
1628 drugs. *Drug Discovery Today* **2012**, *17*, 954–963.
- 1629 (125) Pollard, J. A.; Loken, M.; Gerbing, R. B.; Raimondi, S. C.;  
1630 Hirsch, B. A.; Aplenc, R.; Bernstein, I. D.; Gams, A. S.; Alonzo, T. A.;  
1631 Meshinchi, S. CD33 expression and its association with gemtuzumab  
1632 ozogamicin response: results from the randomized phase III Children’s  
1633 Oncology Group Trial AAML0531. *J. Clin. Oncol.* **2016**, *34*, 747–755.
- 1634 (126) Sievers, E. L.; Larson, R. A.; Stadtmayer, E. A.; Estey, E.;  
1635 Löwenberg, B.; Dombret, H.; Karanes, C.; Theobald, M.; Bennett, J.  
1636 M.; Sherman, M. L.; Berger, M. S.; Eten, C. B.; Loken, M. R.; van  
1637 Dongen, J. J.; Bernstein, I. D.; Appelbaum, F. R. Efficacy and safety of  
1638 gemtuzumab ozogamicin in patients with CD33-positive acute myeloid  
1639 leukemia in first relapse. *J. Clin. Oncol.* **2001**, *19* (13), 3244–3254.
- 1640 (127) Ricart, A. D. Antibody-drug conjugates of calicheamicin  
1641 derivative: gemtuzumab ozogamicin and inotuzumab ozogamicin.  
1642 *Clin. Cancer Res.* **2011**, *17*, 6417–6427.
- 1643 (128) Uy, N.; Nadeau, M.; Stahl, M.; Zeidan, A. M. Inotuzumab  
1644 ozogamicin in the treatment of relapsed/refractory acute B cell  
1645 lymphoblastic leukemia. *J. Blood Med.* **2018**, *9*, 67–74.
- 1646 (129) Doronina, S. O.; Toki, B. E.; Torgov, M. Y.; Mendelsohn, B. A.;  
1647 Cerveny, C. G.; Chace, D. F.; DeBlanc, R. L.; Gearing, R. P.; Bovee, T.  
1648 D.; Siegall, C. B.; Francisco, J. A.; Wahl, A. F.; Meyer, D. L.; Senter, P. D.  
1649 Development of potent monoclonal antibody auristatin conjugates for  
1650 cancer therapy. *Nat. Biotechnol.* **2003**, *21*, 778–784.
- 1651 (130) Hamblett, K. J.; Senter, P. D.; Chace, D. F.; Sun, M. M.; Lenox,  
1652 J.; Cerveny, C. G.; Kissler, K. M.; Bernhardt, S. X.; Kopcha, A. K.;  
1653 Zabinski, R. F.; Meyer, D. L.; Francisco, J. A. Effects of drug loading on  
1654 the antitumor activity of a monoclonal antibody drug conjugate. *Clin.*  
1655 *Cancer Res.* **2004**, *10*, 7063–7070.
- 1656 (131) Schroeder, D. D.; Tankersley, D. L.; Lundblad, J. L. A new  
1657 preparation of modified immune serum globulin (human) suitable for  
1658 intravenous administration. I. Standardization of the reduction and  
1659 alkylation reaction. *Vox Sang.* **1981**, *40*, 373–382.
- 1660 (132) Sharman, J. P.; Wheler, J. J.; Einhorn, L.; Dowlati, A.; Shapiro,  
1661 G. I.; Hilton, J.; Burke, J. M.; Siddiqi, T.; Whiting, N.; Jalal, S. I. A phase  
1662 2, open-label study of brentuximab vedotin in patients with CD30-  
1663 expressing solid tumors. *Invest. New Drugs* **2019**, *37*, 738–747.
- 1664 (133) Sehn, L. H.; Kamdar, M.; Herrera, A. F.; McMillan, A.; Flowers,  
1665 C.; Kim, W. S.; Kim, T. M.; Özcan, M.; Demeter, J.; Hertzberg, M.;  
1666 Trněný, M.; Salles, G. A.; Davies, A.; Hirata, J. H.; Cheng, J.; Ku, G.;  
Mataras, M. J. Randomized phase 2 trial of polatuzumab vedotin (pola) 1667  
with bendamustine and rituximab (BR) in relapsed/refractory (r/r) FL 1668  
and DLBCL. *J. Clin. Oncol.* **2018**, *36* (15), 7507. 1669
- (134) Yu, S.; Pearson, A. D.; Lim, R. K.; Rodgers, D. T.; Li, S.; Parker, 1670  
H. B.; Weglarz, M.; Hampton, E. N.; Bollong, M. J.; Shen, J.; Zambaldo, 1671  
C.; Wang, D.; Woods, A. K.; Wright, T. M.; Schultz, P. G.; Kazane, S. A.; 1672  
Young, T. S.; Tremblay, M. S. Targeted delivery of an anti- 1673  
inflammatory PDE4 inhibitor to immune cells via an antibody-drug 1674  
conjugate. *Mol. Ther.* **2016**, *24*, 2078–2089. 1675
- (135) Yu, S.; Pearson, A.; Lim, R.; Rodgers, D.; Li, S.; Parker, H.; 1676  
Weglarz, M.; Hampton, E.; Bollong, M.; Shen, J.; Zambaldo, C.; Wang, 1677  
D.; Woods, A.; Wright, T.; Schultz, P.; Kazane, S.; Young, T.; Tremblay, 1678  
M. P-262 A PDE4 inhibitor-antibody conjugate for treating ulcerative 1679  
colitis. *Inflammatory Bowel Dis.* **2017**, *23* (1), 262. 1680
- (136) Wang, R. E.; Liu, T.; Wang, Y.; Cao, Y.; Du, J.; Luo, X.; 1681  
Deshmukh, V.; Kim, C. H.; Lawson, B. R.; Tremblay, M. S.; Young, T. 1682  
S.; Kazane, S. A.; Wang, F.; Schultz, P. G. An immunosuppressive 1683  
antibody-drug conjugate. *J. Am. Chem. Soc.* **2015**, *137*, 3229–3232. 1684
- (137) *Chemical Biology: From Small Molecules to Systems Biology and* 1685  
*Drug Design*; Schreiber, L. S., Kapoor, T., Wess, G., Eds.; Wiley-VCH: 1686  
Weinheim, Germany, 2007; Vol. 1-3. 1687
- (138) Jones, L. H.; Bunnage, M. E. Applications of chemogenomic 1688  
library screening in drug discovery. *Nat. Rev. Drug Discovery* **2017**, *16* 1689  
(4), 285–296. 1690
- (139) Hermanson, G. T. *Bioconjugate Techniques*, 3rd ed.; Academic 1691  
Press: San Diego, CA, U.S., 2013. 1692
- (140) Chen, D.; Jansson, A.; Sim, D.; Larsson, A.; Nordlund, P. 1693  
Structural analyses of human thymidylate synthase reveal a site that may 1694  
control conformational switching between active and inactive states. *J.* 1695  
*Biol. Chem.* **2017**, *292*, 13449–13458. 1696
- (141) Durham, T. B.; Blanco, M. J. Target engagement in lead 1697  
generation. *Bioorg. Med. Chem. Lett.* **2015**, *25*, 998–1008. 1698
- (142) Schürmann, M.; Janning, P.; Ziegler, S.; Waldmann, H. Small- 1699  
molecule target engagement in cells. *Cell Chem. Biol.* **2016**, *23*, 435– 1700  
441. 1701
- (143) Rudkouskaya, A.; Sinsuebphon, N.; Ward, J.; Tubbesing, K.; 1702  
Intes, X.; Barroso, M. Quantitative imaging of receptor-ligand 1703  
engagement in intact live animals. *J. Controlled Release* **2018**, *286*, 1704  
451–459. 1705
- (144) Robers, M. B.; Dart, M. L.; Woodroffe, C. C.; Zimprich, C. A.; 1706  
Kirkland, T. A.; Machleidt, T.; Kupcho, K. R.; Levin, S.; Hartnett, J. R.; 1707  
Zimmerman, K.; Niles, A. L.; Ohana, R. F.; Daniels, D. L.; Slater, M.; 1708  
Wood, M. G.; Cong, M.; Cheng, Y. Q.; Wood, K. V. Target engagement and 1709  
drug residence time can be observed in living cells with BRET. *Nat.* 1710  
*Commun.* **2015**, *6*, 10091. 1711
- (145) Stoddart, L. A.; Johnstone, E. K. M.; Wheal, A. J.; Goulding, J.; 1712  
Robers, M. B.; Machleidt, T.; Wood, K. V.; Hill, S. J.; Pflieger, K. D. G. 1713  
Application of BRET to monitor ligand binding to GPCRs. *Nat.* 1714  
*Methods* **2015**, *12*, 661–663. 1715
- (146) Simon, G. M.; Niphakis, M. J.; Cravatt, B. F. Determining target 1716  
engagement in living systems. *Nat. Chem. Biol.* **2013**, *9*, 200–205. 1717
- (147) Copeland, R. A.; Pompliano, D. L.; Meek, T. D. Drug-target 1718  
residence time and its implications for lead optimization. *Nat. Rev. Drug* 1719  
*Discovery* **2006**, *5*, 730–739. 1720
- (148) Tummino, P. J.; Copeland, R. A. Residence time of receptor- 1721  
ligand complexes and its effect on biological function. *Biochemistry* 1722  
**2008**, *47*, 5481–5492. 1723
- (149) Vauquelin, G.; Charlton, S. J. Exploring avidity: understanding 1724  
the potential gains in functional affinity and target residence time of 1725  
bivalent and heterobivalent ligands. *Br. J. Pharmacol.* **2013**, *168*, 1771– 1726  
1785. 1727
- (150) Atkinson, J. M.; Ye, Y.; Gebru, M. T.; Liu, Q.; Zhou, S.; Young, 1728  
M. M.; Takahashi, Y.; Lin, Q.; Tian, F.; Wang, H. G. Time-resolved 1729  
FRET and NMR analyses reveal selective binding of peptides 1730  
containing the LC3-interacting region to ATG8 family proteins. *J.* 1731  
*Biol. Chem.* **2019**, *294* (38), 14033–14042. 1732
- (151) Miller, T. W.; Amason, J. D.; Garcin, E. D.; Lamy, L.; Dranchak, 1733  
P. K.; Macarthur, R.; Braisted, J.; Rubin, J. S.; Burgess, T. L.; Farrell, C. 1734  
L.; Roberts, D. D.; Inglese, J. Quantitative high-throughput screening 1735

- 1736 assays for the discovery and development of SIRP $\alpha$ -CD47 interaction  
1737 inhibitors. *PLoS One* **2019**, *14* (7), No. e0218897.
- 1738 (152) Moreau, M. J.; Morin, I.; Schaeffer, P. M. Quantitative  
1739 determination of protein stability and ligand binding using a green  
1740 fluorescent protein reporter system. *Mol. BioSyst.* **2010**, *6*, 1285–1292.
- 1741 (153) Bücherl, C.; Aker, J.; de Vries, S.; Borst, J. W. Probing protein-  
1742 protein interactions with FRET-FLIM. *Methods Mol. Biol.* **2010**, *655*,  
1743 389–399.
- 1744 (154) Yu, H.; Truong, H.; Mitchell, S. A.; Licican, A.; Gosink, J. J.; Li,  
1745 W.; Lin, J.; Feng, J. Y.; Jürgensmeier, J. M.; Billin, A.; Xu, R.; Patterson,  
1746 S.; Pagratis, N. Homogeneous BTK occupancy assay for pharmacody-  
1747 namic assessment of tirabrutinib (GS-4059/ONO-4059) target  
1748 engagement. *SLAS Discovery* **2018**, *23*, 919–929.
- 1749 (155) Stockmann, H.; Todorovic, V.; Richardson, P. L.; Marin, V.;  
1750 Scott, V.; Gerstein, C.; Lake, M.; Wang, L.; Sadhukhan, R.; Vasudevan,  
1751 A. Cell-surface receptor-ligand interaction analysis with homogeneous  
1752 time-resolved FRET and metabolic glycan engineering: application to  
1753 transmembrane and GPI-anchored receptors. *J. Am. Chem. Soc.* **2017**,  
1754 *139*, 16822–16829.
- 1755 (156) Genovese, F.; Ferrari, S.; Guaitoli, G.; Caselli, M.; Costi, M. P.;  
1756 Ponterini, G. Dimer–monomer equilibrium of human thymidylate  
1757 synthase monitored by fluorescence resonance energy transfer. *Protein*  
1758 *Sci.* **2010**, *19*, 1023–1030.
- 1759 (157) Ponterini, G.; Martello, A.; Pavesi, G.; Lauriola, A.; Luciani, R.;  
1760 Santucci, M.; Pelà, M.; Gozzi, G.; Pacifico, S.; Guerrini, R.; Marverti, G.;  
1761 Costi, M. P.; D’Arca, D. Intracellular quantitative detection of human  
1762 thymidylate synthase engagement with an unconventional inhibitor  
1763 using tetracysteine-diarsenical-probe technology. *Sci. Rep.* **2016**, *6*,  
1764 27198.
- 1765 (158) Di Rocco, G.; Martinelli, I.; Pacifico, S.; Guerrini, R.; Cichero,  
1766 E.; Fossa, P.; Franchini, S.; Cardarelli, S.; Giorgi, M.; Sola, M.;  
1767 Ponterini, G. Fluorometric detection of protein-ligand engagement: the  
1768 case of phosphodiesterase S. *J. Pharm. Biomed. Anal.* **2018**, *149*, 335–  
1769 342.
- 1770 (159) Brown, N. E.; Blumer, J. B.; Hepler, J. R. Bioluminescence  
1771 resonance energy transfer to detect protein-protein interactions in live  
1772 cells. *Methods Mol. Biol.* **2015**, *1278*, 457–465.
- 1773 (160) Koblan, L. W.; Buckley, D. L.; Ott, C. J.; Fitzgerald, M. E.;  
1774 Ember, S. W.; Zhu, J. Y.; Liu, S.; Roberts, J. M.; Remillard, D.; Vittori,  
1775 S.; Zhang, W.; Schonbrunn, E.; Bradner, J. E. Assessment of  
1776 bromodomain target engagement by a series of BI2536 analogues  
1777 with miniaturized BET-BRET. *ChemMedChem* **2016**, *11* (23), 2575–  
1778 2581.
- 1779 (161) Casarini, L.; Riccetti, L.; Limoncella, S.; Lazzaretti, C.;  
1780 Barbagallo, F.; Pacifico, S.; Guerrini, R.; Tagliavini, S.; Trenti, T.;  
1781 Simoni, M.; Sola, M.; Di Rocco, G. Probing the effect of sildenafil on  
1782 progesterone and testosterone production by an intracellular FRET/  
1783 BRET combined approach. *Biochemistry* **2019**, *58*, 799–808.
- 1784 (162) Robers, M. B.; Vasta, J. D.; Corona, C. R.; Ohana, R. F.; Hurst,  
1785 R.; Jhala, M. A.; Comess, K. M.; Wood, K. V. Quantitative, real-time  
1786 measurements of intracellular target engagement using energy transfer.  
1787 *Methods Mol. Biol.* **2019**, *1888*, 45–71.
- 1788 (163) Sartini, S.; Levati, E.; Maccesi, M.; Guerra, M.; Spadoni, G.;  
1789 Bach, S.; Benincasa, M.; Scocchi, M.; Ottonello, S.; Rivara, S.;  
1790 Montanini, B. New antimicrobials targeting bacterial RNA polymerase  
1791 holoenzyme assembly identified with an *in vivo* BRET-based discovery  
1792 platform. *ACS Chem. Biol.* **2019**, *14* (8), 1727–1736.
- 1793 (164) McClure, R. A.; Williams, J. D. Impact of mass spectrometry-  
1794 based technologies and strategies on chemoproteomics as a tool for  
1795 drug discovery. *ACS Med. Chem. Lett.* **2018**, *9*, 785–791.
- 1796 (165) Pan, S.; Jang, S. Y.; Wang, D.; Liew, S. S.; Li, Z.; Lee, J. S.; Yao, S.  
1797 Q. A suite of “minimalist” photo-crosslinkers for live-cell imaging and  
1798 chemical proteomics: case study with BRD4 inhibitors. *Angew. Chem.,*  
1799 *Int. Ed.* **2017**, *56*, 11816–11821.
- 1800 (166) Parker, C. G.; Galmozzi, A.; Wang, Y.; Correia, B. E.; Sasaki, K.;  
1801 Joslyn, C. M.; Kim, A. S.; Cavallaro, C. L.; Lawrence, R. M.; Johnson, S.  
1802 R.; Narvaiza, I.; Saez, E.; Cravatt, B. F. Ligand and target discovery by  
1803 fragment-based screening in human cells. *Cell* **2017**, *168*, 527–541.
- (167) Wang, Z.; Guo, Z.; Song, T.; Zhang, X.; He, N.; Liu, P.; Wang,  
1804 P.; Zhang, Z. Proteome-wide identification of on- and off-targets of Bcl-  
1805 2 inhibitors in native biological systems by using affinity-based probes  
1806 (AfBPs). *ChemBioChem* **2018**, *19*, 2312–2320.
- (168) Wong, M. L.; Murphy, J.; Harrington, E.; Gower, C. M.; Jain, R.  
1808 K.; Schirle, M.; Thomas, J. R. Examining the influence of specificity  
1809 ligands and ATP-competitive ligands on the overall effectiveness of  
1810 bivalent kinase inhibitors. *Proteome Sci.* **2016**, *15*, 17.
- (169) Yang, X.; van Veldhoven, J. P. D.; Offringa, J.; Kuiper, B. J.;  
1812 Lenselink, E. B.; Heitman, L. H.; van der Es, D.; Ijzerman, A. P.  
1813 Development of covalent ligands for G protein-coupled receptors: a  
1814 case for the human adenosine A(3) receptor. *J. Med. Chem.* **2019**, *62*  
1815 (7), 3539–3552.
- (170) Murale, D. P.; Hong, S. C.; Haque, M. M.; Lee, J. S. Photo-  
1817 affinity labeling (PAL) in chemical proteomics: a handy tool to  
1818 investigate protein-protein interactions (PPIs). *Proteome Sci.* **2016**, *15*,  
1819 14.
- (171) Smith, E.; Collins, I. Photoaffinity labeling in target- and  
1821 binding-site identification. *Future Med. Chem.* **2015**, *7* (2), 159–183.
- (172) Hill, J. R.; Robertson, A. A. B. Fishing for Drug Targets: A focus  
1823 on diazirine photoaffinity probe synthesis. *J. Med. Chem.* **2018**, *61* (16),  
1824 6945–6963.
- (173) Kubota, K.; Funabashi, M.; Ogura, Y. Target deconvolution  
1826 from phenotype-based drug discovery by using chemical proteomics  
1827 approaches. *Biochim. Biophys. Acta, Proteins Proteomics* **2019**, *1867* (1),  
1828 22–27.
- (174) Tomohiro, T. Tag-Creation Approaches for Highly Efficient  
1830 Profiling of Interacting Proteins and Domains. In *Photoaffinity Labeling*  
1831 *for Structural Probing Within Protein*; Hatanaka, Y., Hashimoto, M.,  
1832 Eds.; Springer: Tokyo, 2017; pp 13–43.
- (175) Sakurai, K.; Tawa, M.; Okada, A.; Yamada, R.; Sato, N.; Inahara,  
1834 M.; Inoue, M. Active/inactive dual-probe system for selective photo-  
1835 affinity labeling of smallmolecule-binding proteins. *Chem. - Asian J.*  
1836 **2012**, *7*, 1567–1571.
- (176) Zhang, L.; Zhang, Y.; Dong, J.; Liu, J.; Zhang, L.; Sun, H. Design  
1838 and synthesis of novel photoaffinity probes for study of the target  
1839 proteins of oleanolic acid. *Bioorg. Med. Chem. Lett.* **2012**, *22* (2), 1036–  
1840 1039.
- (177) Li, Y. M.; Xu, M.; Lai, M. T.; Huang, Q.; Castro, J. L.; DiMuzio-  
1842 Mower, J.; Harrison, T.; Lellis, C.; Nadin, A.; Neduveil, J. G.; Register,  
1843 R. B.; Sardana, M. K.; Shearman, M. S.; Smith, A. L.; Shi, X. P.; Yin, K.  
1844 C.; Shafer, J. A.; Gardell, S. J. Photoactivated gamma-secretase  
1845 inhibitors directed to the active site covalently label presenilin 1.  
1846 *Nature* **2000**, *405* (6787), 689–694.
- (178) Colca, J. R.; McDonald, W. G.; Cavey, G. S.; Cole, S. L.;  
1848 Holewa, D. D.; Brightwell-Conrad, A. S.; Wolfe, C. L.; Wheeler, J. S.;  
1849 Coulter, K. R.; Kilkuskie, P. M.; Gracheva, E.; Korshunova, Y.;  
1850 Trusgnich, M.; Karr, R.; Wiley, S. E.; Divakaruni, A. S.; Murphy, A. N.;  
1851 Vigueira, P. A.; Finck, B. N.; Kletzien, R. F. Identification of a  
1852 mitochondrial target of thiazolidinedione insulin sensitizers (mTOT)-  
1853 relationship to newly identified mitochondrial pyruvate carrier proteins.  
1854 *PLoS One* **2013**, *8* (5), No. e61551.
- (179) Manzi, L.; Barrow, A. S.; Scott, D.; Layfield, R.; Wright, T. G.;  
1856 Moses, J. E.; Oldham, N. J. Carbene footprinting accurately maps  
1857 binding sites in protein–ligand and protein–protein interactions. *Nat.*  
1858 *Commun.* **2016**, *7*, 13288–13297.
- (180) Horne, J. E.; Walko, M.; Calabrese, A. N.; Levenstein, M. A.;  
1860 Brockwell, D. J.; Kapur, N.; Wilson, A. J.; Radford, S. E. Rapid mapping  
1861 of protein interactions using tag-transfer photocrosslinkers. *Angew.*  
1862 *Chem., Int. Ed.* **2018**, *57* (51), 16688–16692.